https://doi.org/10.1093/plphys/kiae147 PLANT PHYSIOLOGY 2024: 195: 3072–3096

Plant Physiology®

Research Article

A maize semi-dwarf mutant reveals a GRAS transcription factor involved in brassinosteroid signaling

Amanpreet Kaur,[1,2] **Norman B. Best**,[3] **Thomas Hartwig**,[4] **Josh Budka**,[1,2] **Rajdeep S. Khangura**,[1,2] **Steven McKenzie**,[1,2] **Alejandro Aragón-Raygoza**,[5] **Josh Strable**,[5] **Burkhard Schulz**,[6] **Brian P. Dilkes**[1,2,*]

1 Department of Biochemistry, Purdue University, West Lafayette, IN 47907 USA
2 Center for Plant Biology, Purdue University, West Lafayette, IN 47907, USA
3 Plant Genetics Research Unit, USDA-ARS, Columbia, MO 65211, USA
4 Institute for Molecular Physiology, Heinrich-Heine-Universität Düsseldorf, 40225 Düsseldorf, Germany
5 Department of Molecular and Structural Biochemistry, North Carolina State University, Raleigh, NC 27695, USA
6 Department of Plant Science and Landscape Architecture, University of Maryland, College Park, MD 20742, USA

*Author for correspondence: bdilkes@purdue.edu
The author responsible for distribution of materials integral to the findings presented in this article in accordance with the policy described in the Instructions for Authors (https://academic.oup.com/plphys/pages/General-Instructions) is Brian Dilkes.

Abstract

Brassinosteroids (BR) and gibberellins (GA) regulate plant height and leaf angle in maize (*Zea mays*). Mutants with defects in BR or GA biosynthesis or signaling identify components of these pathways and enhance our knowledge about plant growth and development. In this study, we characterized three recessive mutant alleles of *GRAS transcription factor 42* (*gras42*) in maize, a GRAS transcription factor gene orthologous to the *DWARF AND LOW TILLERING* (*DLT*) gene of rice (*Oryza sativa*). These maize mutants exhibited semi-dwarf stature, shorter and wider leaves, and more upright leaf angle. Transcriptome analysis revealed a role for GRAS42 as a determinant of BR signaling. Analysis of the expression consequences from loss of GRAS42 in the *gras42-mu1021149* mutant indicated a weak loss of BR signaling in the mutant, consistent with its previously demonstrated role in BR signaling in rice. Loss of BR signaling was also evident by the enhancement of weak BR biosynthetic mutant alleles in double mutants of *nana plant1-1* and *gras42-mu1021149*. The *gras42-mu1021149* mutant had little effect on GA-regulated gene expression, suggesting that GRAS42 is not a regulator of core GA signaling genes in maize. Single-cell expression data identified *gras42* expressed among cells in the G2/M phase of the cell cycle consistent with its previously demonstrated role in cell cycle gene expression in Arabidopsis (*Arabidopsis thaliana*). *Cis*-acting natural variation controlling GRAS42 transcript accumulation was identified by expression genome-wide association study (eGWAS) in maize. Our results demonstrate a conserved role for GRAS42/SCARECROW-LIKE 28 (SCL28)/DLT in BR signaling, clarify the role of this gene in GA signaling, and suggest mechanisms of tillering and leaf angle control by BR.

Introduction

Plant architecture is a key determinant of plant fitness and crop yield. Above-ground plant architecture influences plant competition, light harvesting, and reproductive capacity. In an agricultural context, manipulating plant height and leaf angle are effective strategies to improve crop yields per unit of land area (Lambert and Johnson 1978; Duvick 2005; Salas Fernandez et al. 2009; Liu et al. 2017; Paciorek et al. 2022).

Received March 14, 2023. Accepted January 18, 2024. Advance access publication May 6, 2024.

A notable example of this is the tremendous increase in wheat (*Triticum aestivum*) and rice (*Oryza sativa*) yields achieved during the 20th century by growing semi-dwarf lodging-resistant varieties (Khush 2001). In maize (*Zea mays*), manipulation of leaf angle has contributed to yield increases by facilitating greater plant densities per unit area (Lambert and Johnson 1978; Liu et al. 2017). Efforts are underway to deploy semi-dwarf maize using the *brachytic2* gene (Bage et al. 2020; Patent 10472684). A comprehensive understanding of the genetic and molecular mechanisms controlling architectural traits will facilitate breeding efforts to improve crop productivity and provide insights into the mechanisms controlling these traits in natural systems.

In maize, above-ground architecture is primarily defined by plant height, ear height, and leaf architecture. Plant height and leaf architecture are regulated by phytohormones, including gibberellins (GAs), brassinosteroids (BRs), and auxins. Maize dwarf mutants have been characterized with defects in GA biosynthesis or signaling, including *dwarf1* (*d1*), *dwarf3* (*d3*), *dwarf5* (*d5*), and *anther ear1* (*an1*) encoded by recessive loss-of-function alleles in biosynthetic enzymes as well as *D8* and *D9* encoded by semi-dominant alleles in the DELLA-domain GRAS transcription factors that regulate GA-associated gene expression (Winkler and Freeling 1994; Bensen et al. 1995; Winkler and Helentjaris 1995; Chen et al. 2014; Fu et al. 2016). These mutations result in short stature, increased tillering, and the retention of anthers in the ear florets. Other dwarf mutants, originally called *nana plants (na)* (Hutchison 1922; Lindstrom 1923; Li 1933), result from BR-deficiency due to loss-of-function mutations in biosynthetic enzymes including *nana plant1 (na1)*, *nana plant 2 (na2)*, and *brassinosteroid-deficient dwarf1* (*brd1*) (Hartwig et al. 2011; Makarevitch et al. 2012; Best et al. 2016). These BR-deficient mutants exhibit short stature, dark green and erect leaves, reduced tillering, and the presence of pistils in the tassel florets. An additional class of dwarf mutants, called *brachytic* (*br*), includes the *br2* mutant defective in the P-glycoprotein1 ABC transporter (Multani 2003). Other maize mutants defective in auxin production have more pleiotropic phenotypes, such as *vanishing tassel 2* (*vt2*), which are semi-dwarf, have a reduced number of leaves, and a severe barren tassel phenotype (Phillips et al. 2011).

Several genes regulating leaf angle have been identified in maize via mutant analysis. The classical maize genes *liguleless1* (*lg1*), *liguleless2* (*lg2*), *liguleless3* (*lg3*), and *rough sheath1* (*rs1*) regulate leaf angle by establishing the blade/sheath boundary (Becraft and Freeling 1994; Fowler and Freeling 1996; Moreno et al. 1997; Walsh et al. 1998; Muehlbauer et al. 1999). Mutations in an APETALA2 (AP2) transcription factor, DWARF & IRREGULAR LEAF (DIL1), lead to dwarf stature and erect leaves (Jiang et al. 2012). The role of BRs in determining leaf angle has been elucidated in Arabidopsis (*Arabidopsis thaliana*), rice (Li et al. 2020; Cao et al. 2022), and in BR loss-of-function mutants of maize including loss of *na1*, *na2*, and *brassinosteroid-deficient dwarf1* (*brd1*), as well as RNAi of *brassinosteroid insensitive1*(*zmbri1*), which all display an erect leaf phenotype indicating a conserved role of BRs in modulating leaf angle (Hartwig et al. 2011; Makarevitch et al. 2012; Kir et al. 2015; Best et al. 2016). Remarkably, many of these genes have subsequently been identified as candidates for natural variation in leaf angle, including *lg1*, *lg2*, and *brd1* (Tian et al. 2019). In addition to finding alleles in genes identified by classical mutagenesis studies, a number of QTLs have been molecularly identified and subsequently linked to these pathways. For example, an allele of *abi2-vp1-transcription factor12/rav-like1* (*abi12/zmravl1*) alters leaf angle by regulating the BR pathway in maize (Tian et al. 2019). Although direct interaction of LG1 with the BR pathway has not been established, DROOPING LEAF1 (DRL1) interacts with LG1 in vitro, which may ultimately repress BRD1 expression and reduce BR levels and leaf angle (Tian et al. 2019). A recent study showed that ZmLG2 targets key transcription factors required for BR signaling, BZR1 (BRASSINAZOLE RESISTANT1), and ZmBEH1 (BZR1/BES1 HOMOLOG GENE1), which further bind to the promoter of a GRAS domain transcription factor, GRAS42 (also known as SCARECROW-LIKE 28 after the name of the ortholog in *Arabidopsis thaliana*), to regulate leaf angle (Wang et al. 2022). BRs also interact with other phytohormones to control leaf angle (Best et al. 2016). GA application increases leaf angle in *na2-1* mutants but not in the wild-type controls, indicating that GA controls leaf angle via an interaction with the BR pathway (Best et al. 2016).

Studies in Arabidopsis have characterized the BR biosynthesis and signaling pathways (Clouse 2011; Chung and Choe 2013; Kim and Russinova 2020). The identification of homologs of several Arabidopsis BR signaling genes in rice suggests conserved mechanisms of BR signaling but our knowledge of BR signaling components in monocots is still limited (Zhang et al. 2014; Kir et al. 2015). In addition, several BR signaling components like DWARF AND LOW TILLERING (DLT), BRASSINOSTEROID UPREGULATED1 (BU1), and TAIHU DWARF1 (TUD1) have been identified through genetic studies in rice (Tanaka et al. 2009; Tong et al. 2009, 2012; Hu et al. 2013; Zhang et al. 2014). Identification of gene functions can help us better understand BR signaling, and the recovery of different genes from mutant screens in monocots as compared to Arabidopsis raises the possibility of distinct signaling mechanisms in monocots. These components have identified additional interactions between hormone pathways. For instance, studies in rice have shown the role for interactions between auxin and BR in leaf angle control, whereas mutants in the auxin-regulated *SMALL ORGAN SIZE1* (*SMOS1*) and *DLT* genes display an epistatic interaction in rice and DLT is required for SMOS1 overexpression to influence plant height and culm width (Hirano et al. 2017; Qiao et al. 2017).

The rice *DLT* gene is a GRAS family transcription factor that acts as a positive regulator of BR signaling (Tong et al. 2009). Rice *dlt* mutants are semi-dwarfs with a reduced number of tillers and short, wide, and more upright leaves. BR biosynthetic gene expression is increased in the *dlt* mutant

indicating that *DLT* is a negative regulator of BR biosynthesis (Tong et al. 2009). The mutants also show altered accumulation of transcripts of BR-regulated genes consistent with the role of *DLT* in BR signaling. The transcription of *DLT* is regulated by a direct interaction of BZR1 with the *DLT* promoter (Tong et al. 2009). At the protein level, DLT is regulated by GLYCOGEN SYNTHASE KINASE2 (GSK2) that phosphorylates both DLT and BZR1 and controls downstream BR signaling (Tong et al. 2012). DLT has also been reported to modulate GA levels in rice (Li et al. 2010). The *d62* mutant allele of *dlt* in rice showed high expression of GA biosynthetic genes and low endogenous GA levels suggesting that DLT plays a role in regulating both hormonal pathways and bridges GA-BR regulation to alter plant architecture. Mutants in the Arabidopsis ortholog of DLT, *SCL28*, dramatically altered cell size, the progression through G2/M phase of cell cycle in root meristems, and the selection of cell division planes (Goldy et al. 2021). A study of maize mutants in the DLT ortholog, *gras42*, also found the mutants had more upright leaves and determined that maize BZR/BEH homologs bind to the *gras42* promoter suggesting that *gras42* acts downstream of BR perception (Wang et al. 2022).

In this study, we identified multiple mutant alleles of the maize ortholog of the rice *DLT* gene, *gras42*. These mutants share a semi-dwarf, reduced tillering, and erect leaves phenotype. We studied the expression consequences of loss of *gras42* to explore its role in BR and GA signaling. While *gras42* acted as a positive regulator of BR-responsive gene expression, it suppressed GA-induced gene expression, and these effects were found to be tissue-specific. A Genome-wide Association study (GWAS) of natural variation in GRAS42 expression identified known BR pathway genes as regulators of *gras42* expression.

Results

Isolation of a *dwarf and low tillering* mutant of maize

The *gras42* gene (Yilmaz et al. 2009) encodes a maize homolog of the rice gene *DLT*, which was identified based on a semi-dwarf low-tillering phenotype (Tong et al. 2009). Maize *gras42* (gene model v5 Zm00001eb378590; v4 Zm00001d045507; v3 AC234164.1_FG004) is found in a syntenic genomic context in maize, rice, and sorghum (*Sorghum bicolor*) and is sister to the AT1G63100/*AtGRAS-8*/*SCARECROW-LIKE 28* (*SCL28*) gene of Arabidopsis in a prior phylogenetic analysis (Guo et al. 2017). A gene disruption in the coding sequence resulting from the insertion of a *Mutator* (*Mu*) element was sequenced as mu10211049 (NCBI accession HQ135270, GI:308313849) as part of the Uniform-*Mu* project (McCarty et al. 2005), and is available through the Maize COOP as *gras42-mu1021149* (Fig. 1). The *Mu* allele, *gras42-mu1021149*, encodes a recessive self-fertile, semi-dwarf mutant with upright crinkled leaves (Fig. 1). Backcrossing the mutant to A619, A632, B73, and W22 resulted in wild-type plants in the F_1 and a 3:1 segregation in the F_2 demonstrating that this mutant phenotype is encoded by a single recessive locus. A similar phenotype was identified segregating as a single monogenic recessive trait among families of the CML247 inbred line (Hartwig 2011). Crosses between the *gras42-mu1021149* and semi-dwarf CML247 individuals failed to complement *gras42-mu1021149* indicating that these were allelic mutants (Hartwig 2011). A third line with similar phenotype was identified in a W22 EMS family generated by Dr. Clifford Weil (03INW22CW0578) among the 2009 field season of the TILLInG project at Purdue University (Till et al. 2004; Weil and Monde 2007). All crosses between these three mutants failed to complement, indicating the phenotypes were recessive and due to alleles at the same gene. Sequencing of the *gras42* allele in the TILLInG line identified a change from tryptophan to stop codon at the 74th codon. The mutator allele was previously described as *brachytic crinkled leaf1* (*bcr1*) (Hartwig 2011) and *upright leaf angle1-1* (*url1-1*) and was also described by Wang et al. (2022), who referred to it as *scl28-1* after the Arabidopsis ortholog, along with a second allele *scl28-2* (*gras42-2*), both of which caused upright leaf angles. We therefore refer to the spontaneous allele from CML247 as *gras42-3* and the EMS allele (03INW22CW0578) as *gras42-4*.

Loss of *gras42* results in short plants with upright and wide leaves

The phenotype of *gras42-mu1021149* was investigated in a segregating F_2 population. The mutants were discernibly different in height from their wild type (WT, *gras42-mu1021149*/+) siblings 26 d after sowing (DAS). This difference in plant height got progressively greater until maturity when homozygous mutants were approximately 60% the height of their wild-type siblings (Fig. 1). The reduced height of the mutant was driven entirely by changes in the internode length, as no differences in node number were noted at maturity (Fig. 1). In addition, the leaves of *gras42-mu1021149* were significantly shorter and wider as compared with wild-type siblings (Fig. 2). Consistent with the overall upright habit of the mutant plants, the leaf angle was more upright and significantly different from wild type for all leaves above the ear node (Fig. 2).

Expression of GRAS42 in wild-type and *gras42-mu1021149* mutant plants

We analyzed publicly available single-cell transcriptomic data from maize vegetative shoot apices (Satterlee et al. 2020) to identify cell clusters enriched for GRAS42 transcripts. Two-cell populations exhibited high accumulation of GRAS42 transcripts (Fig. 3). Using 23 known genes involved in S phase and 190 genes involved in G2/M phase of cell division, clusters of cells corresponding to different phases of cell cycle were marked. The two cell clusters, where the expression of GRAS42 was the highest, were both comprised of G2/M cells (Fig. 3). Further exploration of the two G2/M clusters with high expression of GRAS42

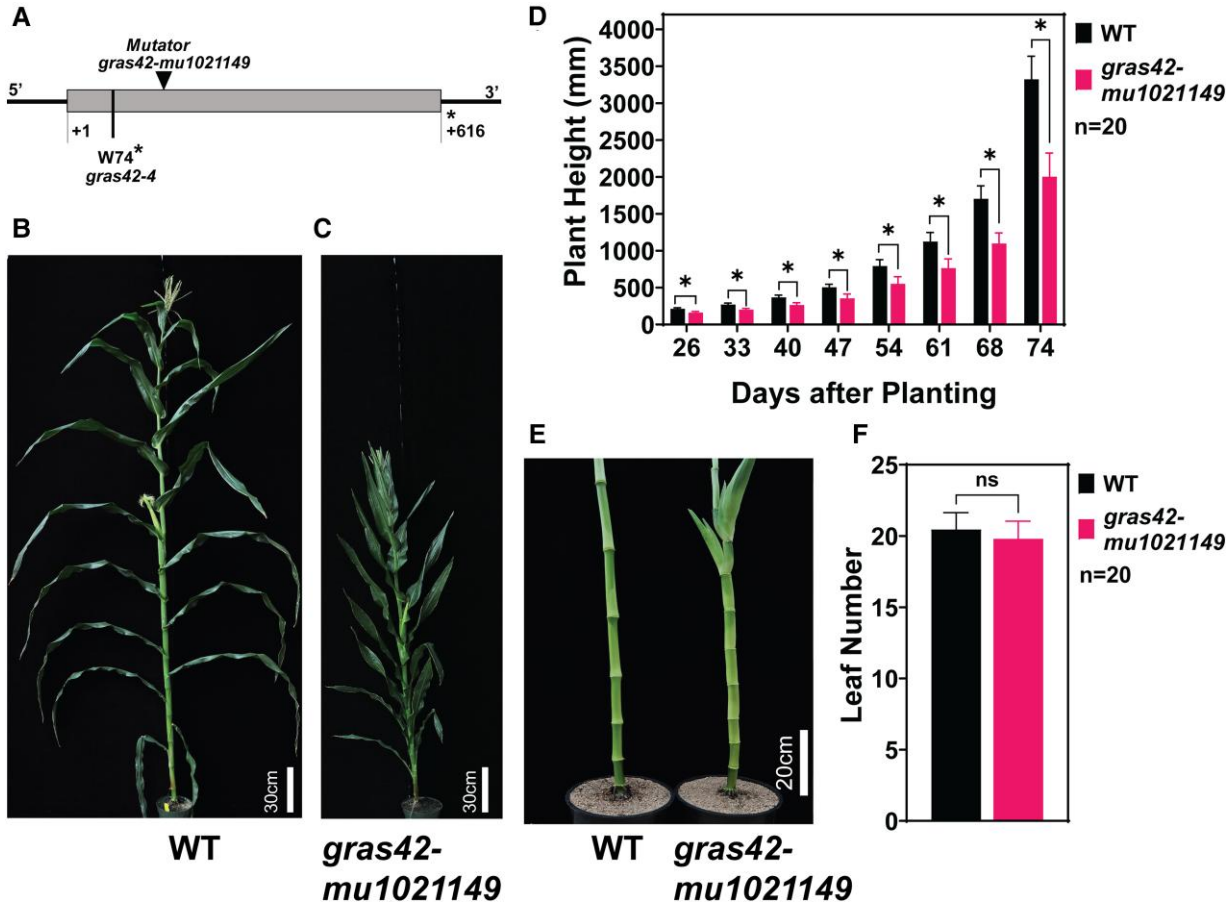

Figure 1. Phenotypic characteristics of *gras42-mu1021149* **A)** Structure of the *gras42* locus (Zm00001d045507) and mutant alleles. Solid gray box depicts the exon. Solid black lines depict 5′ and 3′ untranslated regions. Mutant allele *gras42-mu1021149* is depicted by a triangle at the site of Mutator transposable element insertion and *gras42-4* by a dashed line showing a premature stop codon resulting from a single-nucleotide substitution (G221A). Asterisk indicates a stop codon. First and last amino acid positions of GRAS42 are indicated; **B)** Mature *gras42-mu1021149* heterozygote (*gras42-mu1021149/+;* wild type; WT); **C)** Mature *gras42-mu1021149* homozygote; **D)** Plant height of WT and *gras42-mu1021149*. Error bars are ± SD. Asterisk indicates significant difference between WT and *gras42-mu1021149* determined by Student's t-test ($P < 0.000001$); **E)** Stem and internodes in WT and *gras42-mu1021149*; **F)** Number of leaves in WT and *gras42-mu1021149* siblings. Error bars are ± SD. Significant differences were determined using Student's t-test. ns indicates difference is not significant.

revealed that one of these clusters was enriched in epidermal cells as evidenced by expression of epidermal marker OUTER CELL LAYER4 (OCL4; Zm00001eb024680) (Fig. 3). Within the epidermal marked cells, maize stomatal lineage markers TOO MANY MOUTHS-LIKE1 (TMM1; Zm00001eb159500) and SPEECHLESS2 (ZmSPCH2; Zm00001eb204110) are hypothesized to mark the maize stomatal lineage in all three phases of the cell cycle (Supplementary Fig. S1). GRAS42 expression appears to overlap with these stomatal markers in the epidermal G2/M cell population but is even more differentiated indicating that it is likely expressed during cell divisions that potentially include those leading to stomata. This result was consistent with previously reported investigations of the Arabidopsis homolog, *SCL28*, in roots where expression occurred in G2/M cells and mutants had defects in meristematic epidermal cell walls (Goldy et al. 2021). These results suggest that the consequences of the *gras42-mu1021149* mutant on gene expression should be greatest in RNA samples extracted from tissues that contain a high proportion of actively dividing cells.

We performed RNA sequencing on heterozygous and mutant siblings from an F_1 family of a *gras42-mu1021149/+* x *gras42-mu1021149/gras42-mu1021149* cross. Seedlings were grown to the V3 stage (Abendroth et al. 2011) and RNA was extracted from three separate tissue collections: shoot apices including stem and SAM tissue; expanding leaf sheaths; and the base of the third leaf blade (L3 base). As expected from the single-cell analysis, the abundance of the GRAS42 transcript varied across these three tissues with the highest abundance in the actively dividing shoot apices (Fig. 4) and no expression was detected in RNA extracted from the base of the mature collared L3. These results are similar to *DLT* expression studies in rice where actively dividing and elongating tissues showed the highest expression of DLT transcripts (Tong et al. 2009).

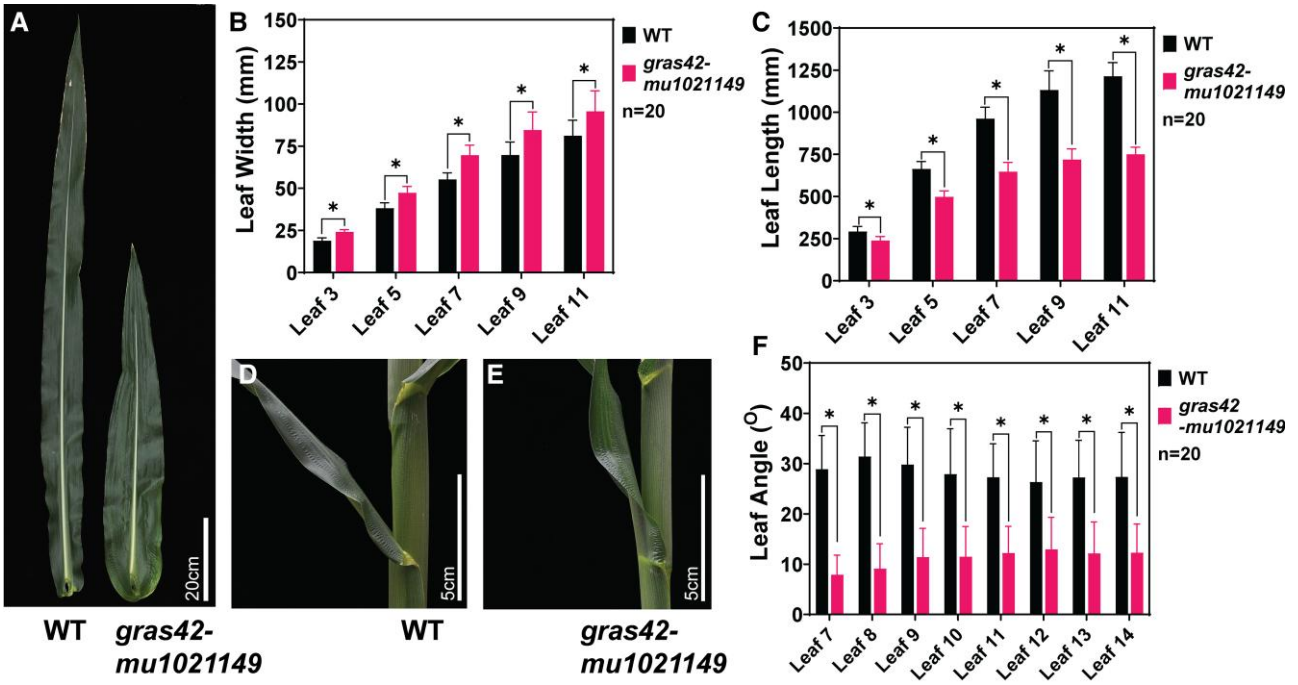

Figure 2. Leaf morphology of *gras42-mu1021149*. **A)** Leaf size of fully extended leaf 15 in heterozygote (WT) and homozygote *gras42-mu1021149*; **B)** Width of leaves in WT and *gras42-mu1021149*; **C)** Length of leaves in WT and *gras42-mu1021149* siblings; **D)** Fully extended leaf 10 in WT; **E)** Fully extended leaf 10 in *gras42-mu1021149*; **F)** Leaf angle (leaf 10) of *gras42-mu1021149* heterozygote and homozygote in degrees (°). The numbers of leaves were counted starting from the base of the plant with the first developing true leaf counted as one. In bar plots, error bars are ± SD. Asterisk indicates significant difference between WT and *gras42-mu1021149* determined by Student's t-test ($P < 0.0001$).

The *Mu* insertion in *gras42-mu1021149* dramatically decreased GRAS42 accumulation in stem and SAM tissue relative to the wild type. We examined the reads in the mutant and wild-type samples and identified that the mutant accumulated transcripts from the transcriptional start site up to the location of the *Mu* element insertion in *gras42-mu1021149*, corresponding to the first third of gene (Supplementary Fig. S2). Some reads did map to the region of the *gras42* gene downstream of the *Mu* insertion but accumulated to a much lower level than seen at the 5′ end upstream of the *Mu* insertion. Furthermore, no junction reads spanning the insertion or read pairs corresponding to a contiguous transcript were identified, suggesting that these 3′ reads derived from promoter activity encoded by the *Mu* element. This indicates that no full-length GRAS42 protein can be encoded by these transcripts. Similar transcript accumulation patterns on either side of the transposon insertion have been observed at other Mu insertions (Ellison et al. 2023). Similar to the effect of the *Mu* insertion on expression in the stem and SAM sample, GRAS42 transcripts in RNA from expanding leaf sheaths displayed a greater proportion of the reads derived from the sequence at 5′ to the *Mu* insertion than the 3′ end (Supplementary Fig. S3).

A paralog of *gras42* in maize

A search for homologs of *gras42* at PLAZA Monocots 5.0 database identified a paralog in maize, *gras47* (Zm00001d041498). Prior phylogenetic studies identified this paralog as also being sister to *SCL28* in Arabidopsis and *DLT* in rice (Guo et al. 2017), suggesting a duplication of this gene in the lineage leading to maize. We performed a phylogenetic analysis of *gras42* homologs in amborella (*Amborella trichopoda*), asparagus (*Asparagus officinalis*), garlic (*Allium sativum*), Arabidopsis, brachypodium (*Brachypodium distachyon*), rice, setaria (*Setaria italica* and *Setaria viridis*), sorghum, and maize. The two paralogs in maize resulted from a maize-lineage duplication that occurred after the divergence of maize and sorghum (Supplementary Fig. S4). We did not detect GRAS47 transcripts in the wild-type samples in our RNA-seq experiment. In addition, we observed no compensatory increase in the expression level of *gras47* in the *gras42-mu1021149* mutant. In addition, transcripts from *gras47* were not detectably expressed (Supplementary Table S1) in 167 of the 173 RNA-seq experiments available in the gene expression database qTeller (Woodhouse et al. 2021b). For experiments in qTeller where both genes were expressed, *gras47* was expressed to a lesser degree than *gras42*. The expression levels of *gras47* suggest that it is likely a pseudogene and does not contribute to plant growth and development. For these reasons, we propose that the phenotypes observed in *gras42-mu1021149* mutant are the result of a loss of *gras42* and not a partial loss phenotype due to the loss of one of two functional copies.

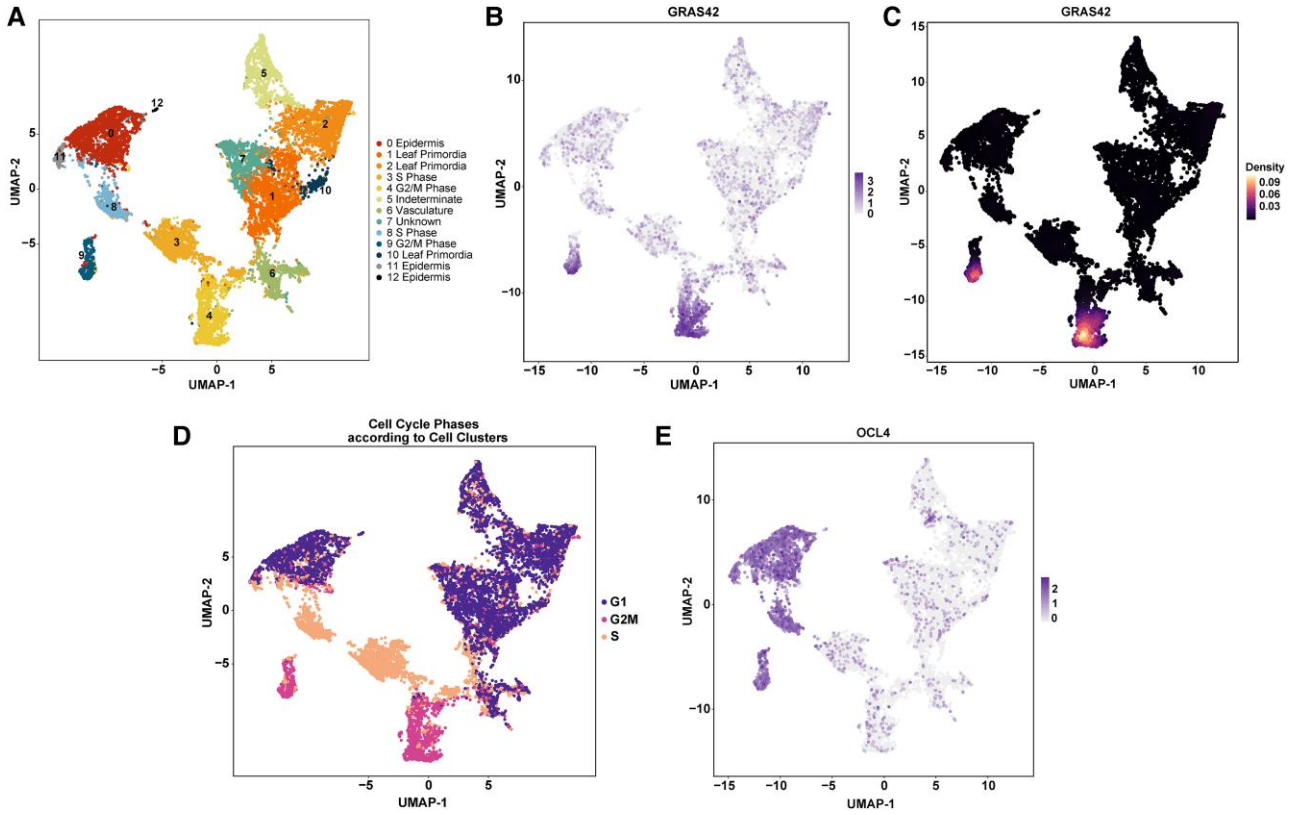

Figure 3. Uniform manifold approximation and projection (UMAP) plots for expression in published single-cell transcriptomic data (Satterlee et al. 2020). **A)** Clusters of cells for different cell types. UMAP identified 13 clusters numbered from 0 to 12 and coded by different colors; **B)** Expression of *gras42* in cell clusters; **C)** Density plot for *gras42;* **D)** Cell cycle phases assessed by gene co-expression; E) Expression of *ocl4* in cell clusters.

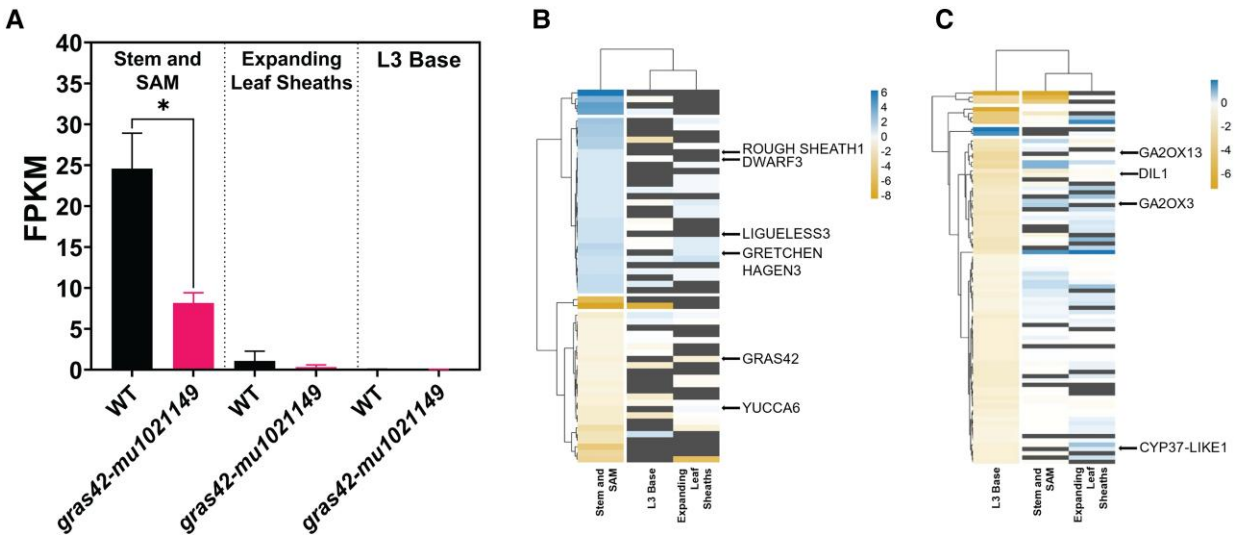

Figure 4. Transcriptomic analysis of *gras42-mu1021149* vs WT (*gras42-mu1021149*/+). **A)** Expression levels (FPKM) of *gras42* gene in WT (*gras42-mu1021149*/+) and *gras42-mu1021149* as detected from RNA sequencing in three tissues: stem and shoot apical meristem (SAM), expanding leaf sheaths and base of third leaf (L3 base). Error bars are ± SD, $n = 3$. Asterisk indicates significant difference between WT and *gras42-mu1021149* determined by Student's t-test (* = $P < 0.05$); **B)** Heatmap showing $\log_2$ fold change of 58 genes differentially expressed in *gras42-mu1021149* stem and SAM tissue across the three tissue types. Blue color indicates genes induced in *gras42-mu1021149*, and gold color represents genes repressed in *gras42-mu1021149* vs WT. Dark gray color represents the genes that were not present in the specific tissue; **C)** Heatmap showing $\log_2$ fold change of 85 genes differentially expressed in *gras42-mu1021149* L3 base compared to wild type across the three tissue types.

RNA-Seq analysis of *gras42-mu1021149* mutant reveals tissue-specific changes in gene expression

We analyzed the RNA sequencing data from homozygous *gras42-mu1021149* mutants and heterozygous controls (phenotypically normal) to identify differentially expressed genes (DEGs). Each of the three tissues sampled at the V3 developmental stage was analyzed separately. The number of significant DEGs (FDR adjusted P-value < 0.05 and $|\log_2\text{-FC}| \geq 1$) in *gras42-mu1021149* as compared to wild type varied in the three tissues, as expected from the tissue-specific variation in GRAS42 accumulation across these three tissues. In stem and SAM, where GRAS42 was expressed (Fig. 4), we identified 58 DEGs, 32 of which were upregulated in *gras42-mu1021149* and 26 were downregulated (Fig. 4). Despite no detectable expression of GRAS42 in the base of L3 (Fig. 4), 85 DEGs were detected, of which 83 were downregulated in *gras42-mu1021149*, and only two were upregulated (Fig. 4). No DEGs were detected in *gras42-mu1021149* in the expanding leaf sheaths despite the expression of GRAS42 in these samples (Fig. 4). The DEGs in stem and L3 base were largely non-overlapping and only two genes were differentially expressed in both tissue samples. The lack of substantial overlap between the DEGs in these tissues indicated that the gene expression consequences of *gras42-mu1021149* are likely tissue-specific. This was also evident from the lack of any consistent pattern in the direction of fold change of the DEGs across the other tissues (Fig. 4). Moreover, the majority of the genes that were altered by *gras42-mu1021149* in stem and SAM were either not expressed or not impacted in the other two tissues (Fig. 4, Supplementary Table S2).

Among the 58 DEGS in the stem including SAM tissue, there were several notable developmental regulators. Genes with altered expression included *rough sheath1* (*rs1*, Zm00001d018742) and *lg3* (Zm00001d040611), both of which are key regulators in leaf angle and development (Becraft and Freeling 1994; Muehlbauer et al. 1999). Both *rs1* and *lg3* are members of class I KNOX family and encode homeodomain proteins (Bolduc et al. 2014). The expression of both genes was only detected in stem (including SAM) but not in the expanding leaf sheaths and L3 base. Dominant gain-of-function *Lg3-O* and *Rs1-O* mutants exhibit blade-to-sheath transformation phenotypes and upright leaf angle. Transcripts from *rs1* and *lg3* were upregulated in *gras42-mu1021149* as compared to wild type suggesting that these genes may be playing a role in the leaf angle phenotype of this mutant. Transcripts encoded by maize *dwarf3* (*d3*, Zm00001d045563), a GA biosynthetic gene, also increased in accumulation in *gras42-mu1021149*. In addition, *gras42-mu1021149* showed a decrease in the accumulation of YUCCA6 (Zm00001d008255) transcripts involved in auxin biosynthesis (Jeong et al. 2007). There was also increased accumulation of transcripts encoded by a paralog of the auxin-responsive and auxin-conjugating enzyme *auxin amido synthase6* which is a member of the *GretchenHagen3* family of proteins (*aas6*, Zm00001d043244) (Aoi et al. 2020).

In *gras42-mu1021149* L3 base, 85 genes were differentially expressed as compared to wild type. The transcript levels of a maize homolog of the constitutive photomorphogenic dwarf gene of Arabidopsis (Ohnishi et al. 2012) encoding a CYP90A1 involved in BR biosynthesis, *cytochrome P450 37-like 1* (*cyp37l1*, Zm00001d004957) were downregulated in *gras42-mu1021149* as compared to wild-type plants. But the gene encoding this enzyme was not affected in stem and expanding leaf sheaths. Genes encoding GA2oxidases (Zm00001d039394, Zm00001d043411), major GA catabolic enzymes, were downregulated in *gras42-mu1021149*. Transcripts from the maize *dwarf & irregular leaf1* (*dil1*, Zm00001d038087) gene, encoding an AP2 transcription factor, were decreased in abundance in *gras42-mu1021149*. The *dil1* mutant is remarkably similar in appearance to *gras42-mu1021149*, and is a semi-dwarf with short, wide, crinkled, and more upright leaves (Jiang et al. 2012). The similarity of these two mutants suggests future experiments to determine if they are in the same pathway.

In Arabidopsis, *SCL28* promotes cell expansion and endoreplication by activating SIAMESE-RELATED (SMR) cyclin-dependent kinase inhibitors (Nomoto et al. 2022). There are 12 SMR paralogs in maize and none of them were among the DEG in any of our three tissues. However, the pattern of *gras42-mu1021149* effects on these genes was non-random in the stem and SAM tissue. All 12 SMR paralogs were decreased in their accumulation in *gras42-mu1021149* as compared to wild-type controls in stem and SAM tissue (Supplementary Table S3). This effect was not consistent across tissues with no discernable effect on accumulation of these genes in expanding leaf sheaths (five up and six down) or L3 base (six up and six down) between *gras42-mu1021149* and wild-type controls.

None of the expression patterns illuminated by the single-cell transcriptome analysis were evident in the DEG sets. We performed a co-regulatory module analysis from the single-cell transcriptomic data and identified the top 200 co-expressed genes with *gras42* (Supplementary Table S4). The genes co-expressed with *gras42* were not enriched among the DEGs in any of the three tissues. This suggests that loss of *gras42* did not disrupt the developmental patterns and cellular identities responsible for co-expression in the single-celled transcriptomic data. Furthermore, as was observed for the SMR genes above, there was no enrichment of core cell cycle regulators among the transcript changes affected by *gras42-mu1021149*. This suggests that the colocalization of GRAS42 transcripts with epidermal markers and the G2M phase of the cell cycle neither predicts its targets nor its role in the control of plant development.

Loss of maize *gras42* does not coordinately impact the expression of GA and BR biosynthetic and core signaling pathway genes

Previous findings in rice have shown enhanced expression of BR biosynthetic genes in rice *dlt* mutants (Tong et al. 2009).

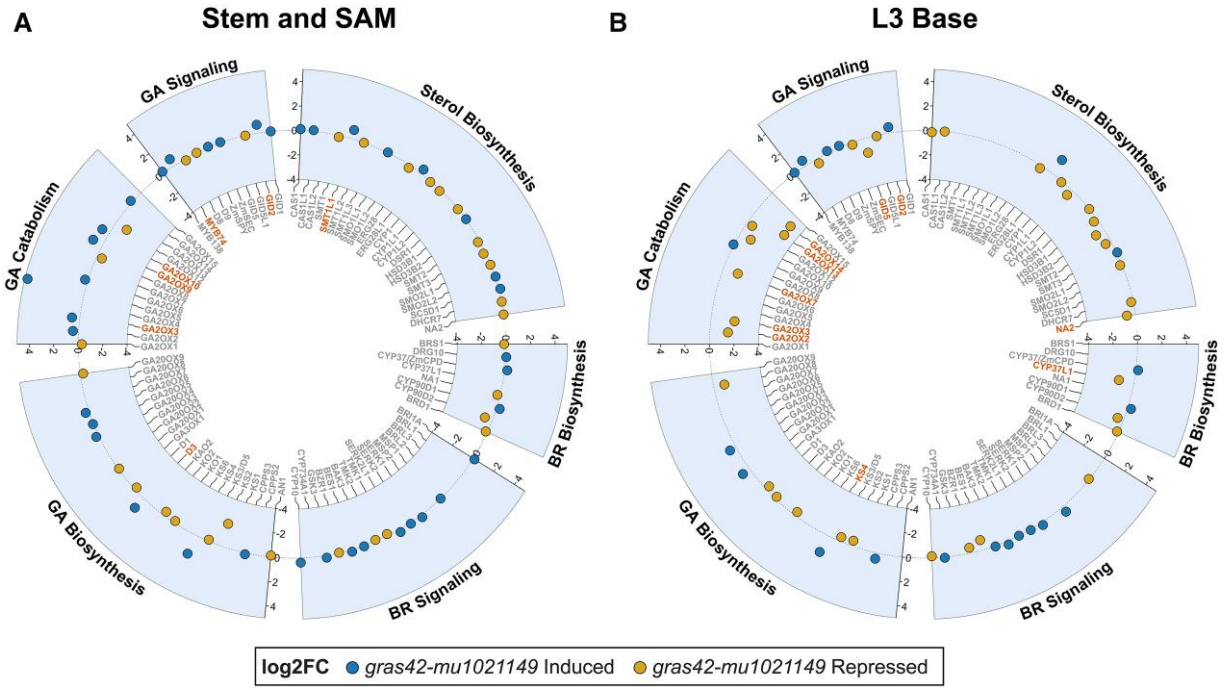

Figure 5. Expression of brassinosteroid (BR) and gibberellin (GA) biosynthetic and core signaling genes in maize *gras42-mu1021149* mutant. Circle plots showing $\log_2$ fold change of BR and GA pathway genes in *gras42-mu1021149* mutant in **A)** stem and shoot apical meristem (SAM) and **B)** base of third leaf (L3 base). Blue dots indicate genes induced in *gras42-mu1021149* as compared to WT and gold dots indicate genes repressed in *gras42-mu1021149*. The genes highlighted in red were significant at unadjusted *P*-value ($P \leq 0.05$) from DEG analysis. The genes in gray were not significant in DEG analysis at $P \leq 0.05$.

In our RNA-seq analysis, the CYP37L1 (Zm00001d004957) transcript was identified as a DEG in L3 base RNA (Fig. 5), but no other BR biosynthetic genes were identified as DEG in *gras42-mu1021149* even at a more relaxed nominal *P*-value < 0.05 cutoff in any of the three tissues (Fig. 5 and Supplementary Fig. S5). We extended the analysis to include sterol biosynthetic genes and only identified the *sterol methyltransferase1-like1* (*smt1l1*, Zm00001d013035) gene as differentially expressed in *gras42-mu1021149* and only in stem and SAM samples. In addition, no genes with known roles in BR signaling (e.g. maize homologs of *BRI1*, *BZR1*, *GSK1*, *BES1*) were differentially expressed even at a relaxed cutoff of an uncorrected *P*-value < 0.05 in comparisons between *gras42-mu1021149* and heterozygous controls (Fig. 5 and Supplementary S5). These findings indicate that maize *gras42* is not a key regulator of transcription for genes in sterol or BR biosynthesis and signaling.

Li et al. (2010) demonstrated that the rice *dlt* mutant, *d62*, had reduced endogenous levels of GA_1 and increased expression of GA biosynthetic genes. We examined our maize *gras42-mu1021149* RNA-seq experiments for changes in transcript levels of the maize orthologs to the GA biosynthetic genes *cps1* (*ent-copalyl diphosphate synthase 1*), *ks1* (*ent-kaurene synthase 1*), *ko1* (*ent-kaurene oxidase 1*), *kao1* (*ent-kaurenoic acid oxidase 1*), and *ga2oxidases* (Supplementary Table S5). To reduce the false negative rate inherent in transcriptome-wide false discovery rate controls (used above in the DEG analysis) we used an unadjusted *P*-value below 0.05 to determine the statistical significance of these genes for differential expression. This had very little effect on the detection of differential gene expression, indicating that the GA pathway was not the main target of GRAS42 in maize. As mentioned above, and similarly to rice *d62*, the kaurene oxidase encoded by *d3* (Zm00001d045563) was increased in abundance in the *gras42-mu1021149* stem and SAM samples (Fig. 5, Supplementary Table S5). However, there was no significant change in the transcript levels of any of the other GA biosynthetic genes in *gras42-mu1021149* relative to wild type in this tissue. Furthermore, *gras42-mu1021149* had tissue-specific effects on gene expression and no consistent pattern of gene expression effects on these genes was detected (Fig. 5). The other significant DEG in our data were *ga2oxidases*, *ga2ox3*, *ga2ox9*, and *ga2ox10* (Zm00001d043411, Zm00001d008909, and Zm00001d012712, respectively), where loss of *gras42-mu1021149* resulted in increased expression (Fig. 5, Supplementary Table S5). No changes in GA biosynthetic genes were noted in expanding leaf sheaths (Supplementary Fig. S5). A number of *ga2oxidases* (*ga2ox2* [Zm00001d002999], *ga2ox3*, *ga2ox7* [Zm00001d038695], *ga2ox13* [Zm00001d039394], and *ga2ox14* [Zm00001d035994]) were impacted by *gras42-mu1021149* in L3 base but the effect was in the opposite direction as observed in the stem and SAM samples demonstrating no consistent pattern for the loss of *gras42* on GA biosynthetic gene expression (Fig. 5).

Table 1. Distribution of *gras42-mu1021149* effects on gene expression for the set of differentially expressed genes in leaf tissue treated with brassinosteroid (BR)

gras42-mu1021149 Tissue	Gene set: BR effect in leaves	Observed (*gras42-mu1021149* vs WT)			Expected (*gras42-mu1021149* vs WT)		Chi-Square *P*-value
		Up	Down	Total	Up	Down	
Stem and SAM	BR induced	488	592	1080	534.0	546.0	0.005
	BR repressed	231	117	348	172.1	175.9	2.6E-10
Expanding Leaf Sheaths	BR induced	522	564	1086	537.1	548.9	0.36
	BR repressed	238	110	348	172.1	175.9	1.6E-12
L3 Base	BR induced	398	676	1074	570.8	503.1	4.2E-26
	BR repressed	188	171	359	190.8	168.2	0.77

The *an1* (Zm00001d032961) gene, which encodes the copalyl diphosphate synthase required for GA biosynthesis, was also decreased in abundance in L3 base samples (Fig. 5). While it is possible that *gras42* is involved in maintaining GA homeostasis in maize, the lack of correspondence in gene expression effects between tissues suggest that this is not the primary role for this transcription factor.

The expression of GA signaling genes was also examined. Transcript abundance of the two DELLA-domain GRAS transcription factor encoding genes, *d8* (Zm00001d033680) and *d9* (Zm00001d013465), was not affected by loss of GRAS42 in any tissue. The levels of GIBBERELLIN-INSENSITIVE DWARF PROTEIN HOMOLOG2 (GID2, Zm00001d010308) transcripts, which encode a GA receptor homologous to Arabidopsis GID1A, were upregulated in *gras42-mu1021149* relative to the wild type in stem and SAM and L3 base experiments but were unaffected in the expanding leaf sheaths (Fig. 5 and Supplementary Fig. S5). In addition, loss of *gras42-mu1021149* led to increased accumulation of transcripts encoded by *myb74* (Zm00001d012544) in stem and SAM tissue. The only other GA signaling gene that was differentially expressed in *gras42-mu1021149* was *gid5* (Zm00001d016973). The accumulation of transcripts from *gid5*, homolog of Arabidopsis *SLEEPY1 (SLY1)*, was significantly reduced in *gras42-mu1021149* L3 base but not affected in the other two tissues (Fig. 5, Supplementary Fig. S5, and Supplementary Table S5). Similar to the GA biosynthetic genes, our data suggest that *gras42* does not affect the transcript abundances of core GA signaling genes.

gras42-mu1021149 enhances the expression of genes suppressed by BR

The three mutant alleles of *gras42* (*gras42-mu1021149*, *gras42-3*, *gras42-4*) are all short with erect leaves. These phenotypes are similar to, but much weaker than, maize BR-deficient *brd1*, *na1-1*, and *na2-1* mutant phenotypes (Hartwig et al. 2011; Makarevitch et al. 2012; Best et al. 2016). To explore the possibility that *gras42* influences BR-responsive gene expression independent of altering BR biosynthesis or signaling transcript abundance, we looked at the effect of the loss of *gras42* on a set of BR-responsive genes. The list of DEGs that responded to treatment with excess BR from leaf and shoot tissues were obtained from previously published work (Trevisan et al. 2020). These consisted of 1,124 genes increased and 377 genes decreased in expression in leaves when treated with BR and 30 genes increased and 192 genes decreased in shoots treated with BR (Trevisan et al. 2020). These genes were analyzed as a set to determine if *gras42-mu1021149* had a non-random effect on the direction of expression via chi-squared analyses.

In stem and SAM tissue, loss of GRAS42 in *gras42-mu1021149* led to non-random changes in the expression of genes that were previously identified to be differentially expressed following treatment with BR. Overlapping the genes in our RNA-seq analysis with the set of BR-induced genes in maize leaves (Trevisan et al. 2020) identified 1,080 genes in common. Of these, 488 were accumulated and 592 were decreased in abundance consistent with a weak loss of BR response in *gras42-mu1021149* SAM tissue (chi-squared *P*-value = 0.005; Table 1). Overlapping our RNA-seq analysis with the genes suppressed by the treatment of leaves with BR (BR-repressed genes) identified 348 genes also present in our stem and SAM tissue. Of these transcripts, 231 were increased in *gras42-mu1021149* and 117 were decreased in accumulation (chi-squared *P*-value = 2.62E-10). This non-random pattern among the BR-repressed genes was also consistent with a weak loss of BR responsiveness in *gras42-mu1021149* SAM tissue. Very few genes were increased in expression in shoot tissue following treatment with BR (Trevisan et al. 2020) and no chi-squared tests were significant for this gene list (Table 2). Among the genes repressed by BR in the sheath and shoot tissue, we identified 149 genes in our RNA-seq experiment with stem and SAM tissues. Of these, a 2:1 ratio (100:49; Table 1) were increased in their accumulation in *gras42-mu1021149*. This, again, demonstrated a loss of BR-responsive gene expression in *gras42-mu1021149* mutants. A similar pattern was observed for leaf and shoot BR-repressed genes in *gras42-mu1021149* expanding leaf sheaths (Tables 1 and 2) indicating that *gras42-mu1021149* fails to suppress the expression of BR-repressed genes. This indicates a role for *gras42* in at least a subset of genes effected by BR treatment.

In L3 base, we identified 1,074 genes overlapping with the leaf BR-induced genes (Trevisan et al. 2020), 63% of which were suppressed by loss of GRAS42 consistent with weak

Table 2. Distribution of *gras42-mu1021149* effects on gene expression for the set of differentially expressed genes in stem and leaf sheath tissue treated with BR

gras42-mu1021149 Tissue	Gene set: BR effect in shoot and leaf sheaths	Observed (*gras42-mu1021149* vs WT)			Expected (*gras42-mu1021149* vs WT)		Chi-Square *P*-value
		Up	Down	Total	Up	Down	
Stem and SAM	BR induced	11	10	21	10.4	10.6	0.79
	BR repressed	100	49	149	73.7	75.3	1.6E-05
Expanding Leaf Sheaths	BR induced	9	12	21	10.4	10.6	0.55
	BR repressed	118	33	151	74.7	76.3	1.7E-12
L3 Base	BR induced	9	11	20	10.6	9.4	0.47
	BR repressed	41	98	139	73.9	65.1	2.3E-08

Table 3. Distribution of *gras42-mu1021149* effects on gene expression for the set of differentially expressed genes in leaf sheath tissue treated with gibberellin (GA)

gras42-mu1021149 Tissue	Gene set: GA effect in leaf sheath	Observed (*gras42-mu1021149* vs WT)			Expected (*gras42-mu1021149* vs WT)		Chi-Square *P*-value
		Up	Down	Total	Up	Down	
Stem and SAM	GA induced	144	94	238	117.7	120.3	0.00064
	GA repressed	39	34	73	36.1	36.9	0.47
Expanding Leaf Sheaths	GA induced	187	51	238	117.7	120.3	2.6E-19
	GA repressed	28	46	74	36.6	37.4	0.046
L3 Base	GA induced	52	183	235	124.9	110.1	1.5E-21
	GA repressed	29	45	74	39.3	34.7	0.016

loss of BR responsiveness. However, a divergent pattern was observed for the genes repressed by BR in shoot (Trevisan et al. 2020) and our L3 base RNA-seq experiment (Table 2). In this tissue, *gras42-mu1021149* led to an effect on gene expression that resembled a gain of BR signaling. This was manifested as 41 BR-repressed genes increasing and 98 BR-repressed genes decreasing in abundance in the L3 base samples of *gras42-mu1021149* relative to wild-type controls. As shown previously, *gras42* is not expressed in L3 base (Fig. 4) and is predominantly expressed in dividing cells (Fig. 3). Thus, the consequences on gene expression are likely to be a secondary effect of the loss of *gras42* elsewhere in the plant.

GRAS42 is a suppressor of GA-induced gene expression

Though the *gras42-mu1021149* mutant did not act through transcription of genes in GA signaling or synthesis, we tested if it was a regulator of GA signal transduction. To examine the impact of loss of *gras42* on GA-responsive gene expression, we obtained genes differentially expressed in wild-type maize leaf sheaths (V3 stage) upon GA treatment from a previously published study (Wang et al. 2019). This dataset comprised 254 genes induced, and 81 genes repressed upon GA treatment. Of the 254 GA-induced genes in leaf sheath (Wang et al. 2019), we identified 238 genes present in our RNA sequencing in stem and SAM as well as expanding leaf sheaths and 235 in L3 base (Table 3). GA-induced genes were non-randomly affected by loss of *gras42* in stem and SAM consistent with greater GA responses in *gras42-mu1021149* mutants. Of the 238 GA-induced genes, 144 transcripts were increased and 94 decreased in abundance *gras42-mu1021149* as compared to wild type. On the other hand, in the data from expanding leaf sheaths, where our RNA-seq data are the tissue closest to that used in the previous GA treatment experiment (Wang et al. 2019), transcript levels of 187 GA-induced genes were higher in *gras42-mu1021149* and 51 were lower as compared to wild type. The *gras42-mu1021149* mutant had no effect on the direction of expression for GA-repressed genes in our stem and SAM RNA-seq data set. Expanding leaf sheath data did show a non-random distribution where 46 of the 74 GA-repressed genes were suppressed in *gras42-mu1021149* as compared to wild type. These expression patterns were consistent with an excess GA response in this mutant, suggesting that *gras42* encodes a negative regulator of GA signaling in these two tissue types.

Interestingly, the gene expression pattern affected by *gras42-mu1021149* for GA-induced genes in L3 base was opposite to that observed in the other two tissues. Among the 235 GA-induced genes, transcript abundance of 183 decreased in *gras42-mu1021149* indicating that the mutant gene expression pattern in this tissue resembles a loss of GA. This divergent behavior of L3 base from other two tissues is somewhat similar to our previous observations with shoot BR-repressed genes and may reflect the secondary impact of the mutant in this tissue where GRAS42 was not accumulated (Fig. 4).

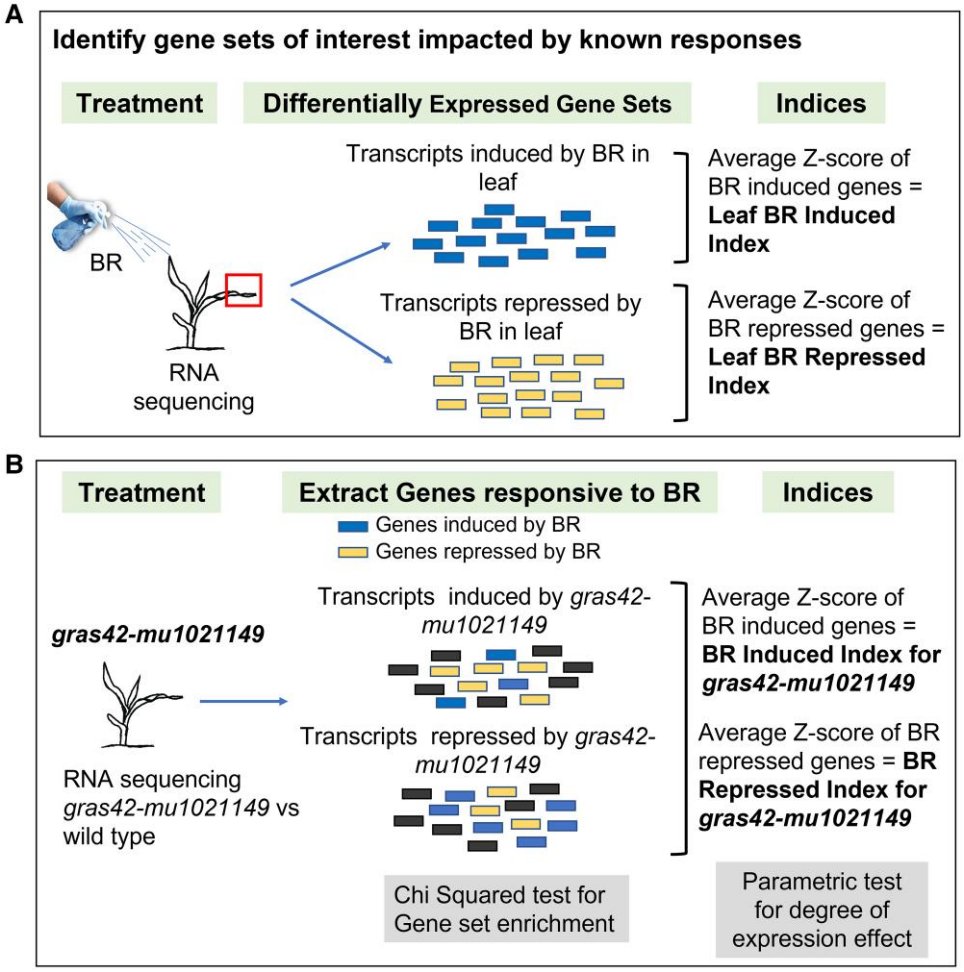

Figure 6. Schematic for Index calculation. **A)** The first step is to identify the gene sets impacted by known responses. In this example, genes differentially expressed in leaf tissue upon brassinosteroid (BR) treatment formed the two BR-responsive gene sets. Genes with increased transcripts in BR-treated samples were referred to as leaf BR-induced genes and those with decreased transcript counts after BR treatment were referred to as leaf BR-repressed genes. A z-score was calculated for each gene in the two (mock-treated and BR-treated) samples. Average of the z-scores for all the genes enhanced by BR treatment gives a single value (Leaf BR-induced index) that reports positive response to excess BR. Likewise, Leaf BR-repressed index summarizes the decreased expression in response to excess BR. **B)** Expression patterns of BR-responsive gene sets identified above were analyzed in *gras42-mu1021149* to assess the status of BR signaling in *gras42-mu1021149*. The counts of BR-induced transcripts (and BR-repressed transcripts) enhanced or repressed by *gras42-mu1021149* were analyzed by chi-square test. The z-scores of leaf BR-responsive genes were calculated from the normalized counts in WT and *gras42-mu1021149*. The average of z-scores for each gene set in *gras42-mu1021149* resulted in index values that summarize BR response in *gras42-mu1021149*.

Gene expression identifies leaf sheath as BR-responsive tissue and *gras42* as a suppressor of BR-repressed genes

We created a parametric summary statistic to complement the gene set tests carried out by chi-squared tests (Tables 1, 2, and 3). To create a single value to report the response status of a transcriptional data set for BR or GA signaling, we calculated an average of the Z-scores for all DEGs that responded to each treatment by significantly increasing or decreasing in abundance. This turned each set of DEGs into a single value reporter of that treatment's signaling status in the tissues sampled for gene expression analysis (Fig. 6). These index values aggregate the response of maize genes to excess BRs or GA. Any significant change in these indices in *gras42-mu1021149* as compared to wild-type controls will give us an indication of the activation state of the BR or GA response pathways in *gras42-mu1021149* mutants.

A summary of the positive response to BR excess in the leaf was constructed using the set of transcripts that increased in abundance upon BR treatment of wild-type maize (Trevisan et al. 2020). The Z-scores of the normalized counts for these genes were calculated using all replicates from wild type and *gras42-mu1021149* across our RNA-seq experiments (Fig. 6). The value, a leaf "BR-induced index" (Fig. 6), for each genotype was generated by taking the mean Z-score of these genes. If the gene expression pattern in that sample resembles the

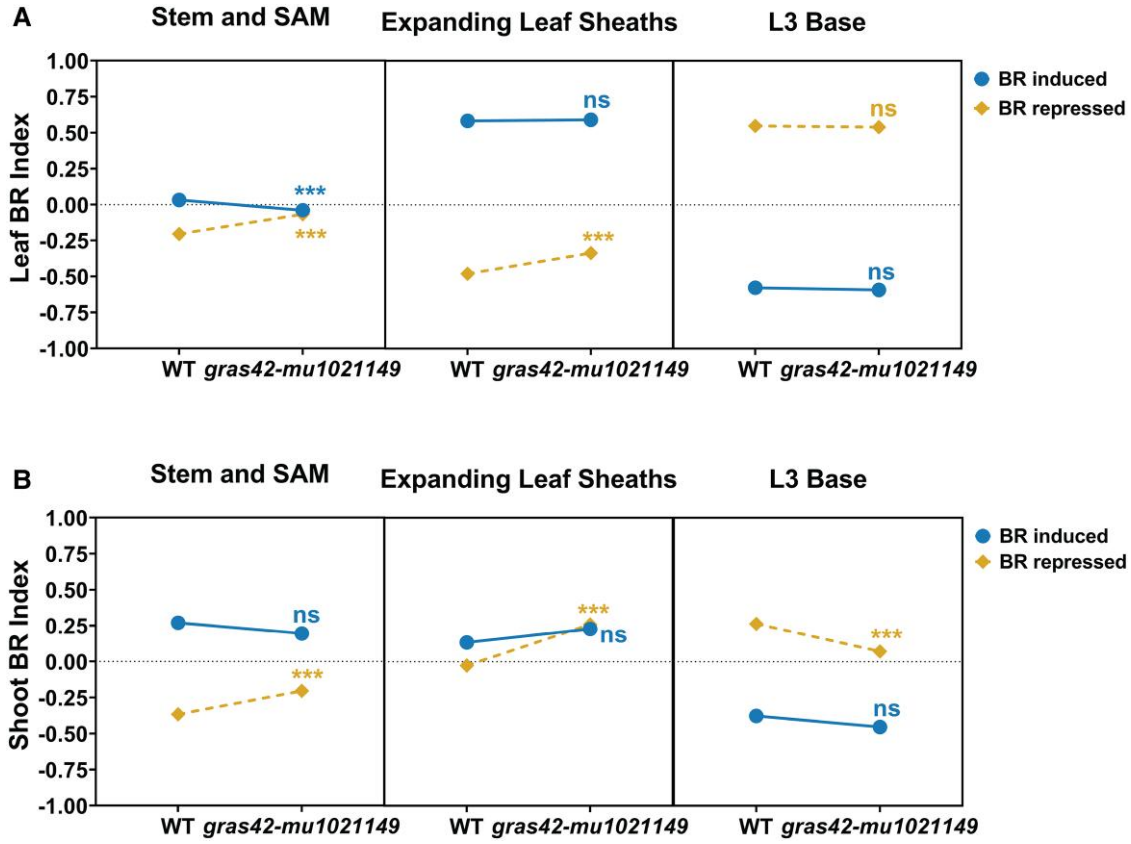

Figure 7. Brassinosteroid (BR) indices in wild type (WT) and *gras42-mu1021149* across three tissues (stem and shoot apical meristem [SAM], expanding leaf sheaths and base of third leaf [L3 base]). **A)** Leaf BR-induced index (Solid blue line with circle) comprises 1,104 genes enhanced by BR treatment and Leaf BR-repressed index (solid yellow line with diamond) represents 374 genes repressed by BR treatment; **B)** Shoot BR-induced index (Solid blue line with circle) comprises 21 genes enhanced by BR treatment and Shoot BR-repressed index (dashed yellow line with diamond) represents 190 genes repressed by BR treatment. A student's t-test was performed to determine the significant differences between the three replicates of WT and *gras42-mu1021149* profiled by RNA-Seq. ns, not significant; ***$P < 0.001$.

coordinated increase in BR-induced genes, this index value will increase. If the expression pattern resembles a loss of BR signaling, this value will decrease. This value reports the similarity of any sample's gene expression pattern to BR-induced gene expression. Likewise, an index value summarizing the genes repressed by BR excess, the leaf "BR-repressed index", was calculated from the average change in expression in our experiments for all transcripts significantly suppressed by BR treatment in the leaf tissue (Trevisan et al. 2020). Similar indices were calculated using BR-responsive genes in shoot tissue (Trevisan et al. 2020).

The comparison of BR indices in *gras42-mu1021149* and wild-type siblings allowed us to predict the status of BR responsiveness in the mutant (Fig. 7). Loss of *gras42* led a reduction in BR-induced genes (Leaf BR-induced index) an increase in BR-repressed genes (Leaf BR-repressed index). This weak loss of BR signaling in *gras42-mu1021149* is similar to that observed by the chi-squared set enrichment analysis (Table 1). The leaf BR-repressed index also increased in *gras42-mu1021149* expanding leaf sheaths consistently indicating a weak loss of BR signaling in *gras42-mu1021149*. In L3 base, neither of the two leaf BR indices showed any significant changes (Fig. 7) consistent with the lack of *gras42* gene expression in this tissue (Fig. 4). The BR-induced index calculated from shoot RNA data (Shoot BR-induced index) was not impacted by loss of *gras42* in any of the three tissues. Very few genes ($n = 21$) were induced by BR excess in the shoot experiment, resulting in low power to detect significant changes in gene expression across our experiments. The shoot BR-repressed index comprised 149 genes and therefore provides a better estimate of expression effects. Similar to the leaf BR-repressed index, the Shoot BR-repressed index increased in the *gras42-mu1021149* mutant stem and SAM as well as in expanding leaf sheaths (Fig. 7). This once again demonstrated reduced BR responses in the *gras42-mu1021149* mutants. All results were coherent with the chi-squared test observations and demonstrate that *gras42* is a positive regulator of BR signaling in maize stem and expanding leaf sheaths where *gras42* is expressed. The stronger effect on genes repressed by BR may indicate that *gras42* acts as a negative regulator of the genes repressed by BR signal transduction.

The shoot BR-repressed index showed a significant reduction in *gras42-mu1021149* as compared to wild type in L3 base (Fig. 7) suggesting a possible increase in BR signaling. This was similar to what was observed in the chi-squared

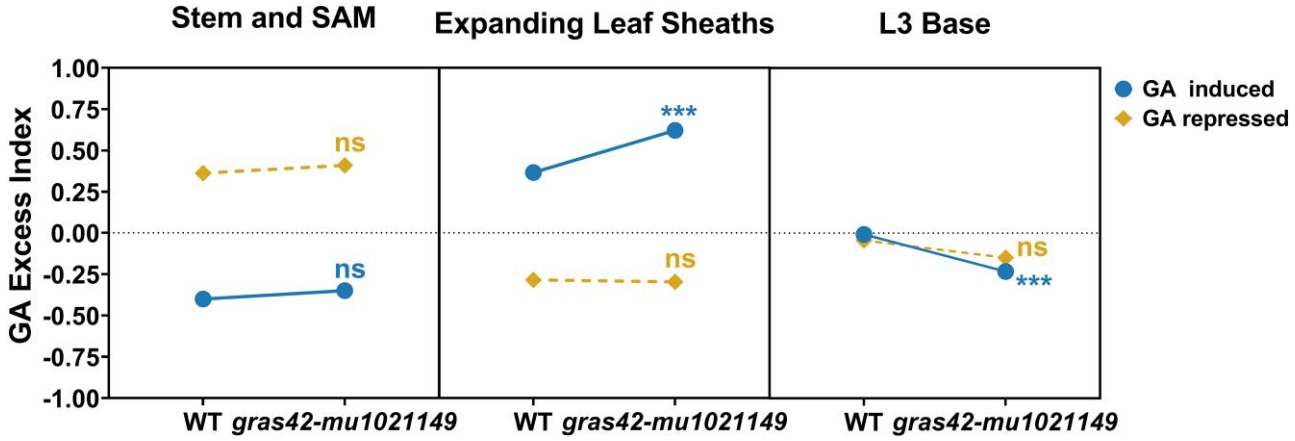

Figure 8. Gibberellin (GA) indices in wild type (WT) and *gras42-mu1021149* across three tissues (stem and shoot apical meristem [SAM], expanding leaf sheaths and base of third leaf [L3 base]). GA-induced index (Solid blue line with circle) comprises 242 genes enhanced by GA treatment and GA-repressed index (dashed yellow line with diamond) represents 75 genes repressed by GA treatment. A student's t-test was performed to determine the significant (*P*-value <0.05) differences between the three replicates of WT and *gras42-mu1021149* profiled by RNA-Seq. ns, not significant; ***$P < 0.001$.

analysis of the BR-regulated gene sets in the L3 base RNA-seq experiment (Tables 1 and 2). The absence of GRAS42 accumulation in L3 base (Fig. 4) and accumulation in actively dividing cells (Fig. 3) suggests that any effects observed in these experiments are likely indirect effects of defects in mutant growth or mobile signals from other parts of the plant.

Comparison of these indices across the wild-type control tissues can also be used to explore differences in the relative activities of BR responses as a result of maize development. Comparing the BR-induced and BR-repressed indices in wild-type samples revealed tissue-specific effects on the state of BR-responsive genes (Fig. 7). The two Leaf BR indices indicate positive BR signaling in wild-type leaf sheath and stem and SAM samples, but not L3 Base (Fig. 7). A similar expression pattern was observed using the indices calculated from the shoot BR treatments (Fig. 7). These results suggest greater BR response in these tissues either from greater BR levels or more sensitive signaling. The leaf sheath sample had index values consistent with the highest BR signaling levels among these three tissues. Remarkably, in wild-type L3 base samples the expression of BR-repressed genes (Leaf BR-repressed index) was higher than the expression of BR-induced genes (Leaf BR-induced index) (Figure 7). A similar result was evident by the distribution of shoot BR-induced and shoot BR-repressed indices in L3 base (Fig. 7). This suggests repression of BR-induced genes in the fully expanded leaf tissue and may contribute to the opposing patterns seen for these gene sets in L3 base as compared to the two actively growing tissues (Tables 1 and 2 and Fig. 7).

Gene expression identifies leaf sheath as high GA and rules out *gras42* as a core GA signaling gene

Index values reporting GA-responsive transcripts were calculated using the DEGs identified following GA excess treatment of maize seedlings (Wang et al. 2019). This permitted comparison of GA pathway activation status across the three wild-type maize tissues. Gene expression in the wild-type stem and SAM sample exhibited lower expression of GA-induced genes and higher expression of GA-repressed genes than the other two samples, indicating low GA response in this tissue. The rapidly elongating tissue of the expanding leaf sheaths, by contrast, showed the highest GA signaling of the three samples (Fig. 8).

Loss of *gras42* increased the GA-induced index value in expanding leaf sheaths. This suggests excess GA signaling in this mutant in this tissue. In the L3 base samples, however, the GA-induced index was reduced in *gras42-mu1021149* indicating a reduced GA signaling by this mutant in this tissue. Given the very low expression of *gras42* in our leaf samples and preferential accumulation in actively dividing cells (Fig. 4 and Fig. 3), this may be an indirect effect of the mutant. No effect was observed for either index in the stem and SAM RNA-seq experiments. Taken together with the chi-squared analysis, the inconsistency of the response across tissues and weak effects suggests that *gras42* is not a core regulator of GA signaling in maize.

Loss of *gras42* influences the phenotype of GA and BR biosynthetic mutants

We carried out a genetic test of whether the observed differences in hormone-regulated gene expression, were part of the mechanism of altered growth and development in the *gras42-mu1021149* mutant by generating double mutants of *gras42-mu1021149* with *na1-1* and *d1*. The *na1-1* mutant is a classical maize dwarf carrying a mutation in the homolog of Arabidopsis *DE-ETIOLATED2* (*DET2*), encoding *sterol 5-alpha reductase*, a key enzyme in BR biosynthesis (Hartwig et al. 2011). The *na1-1* mutants have short, dark green leaves,

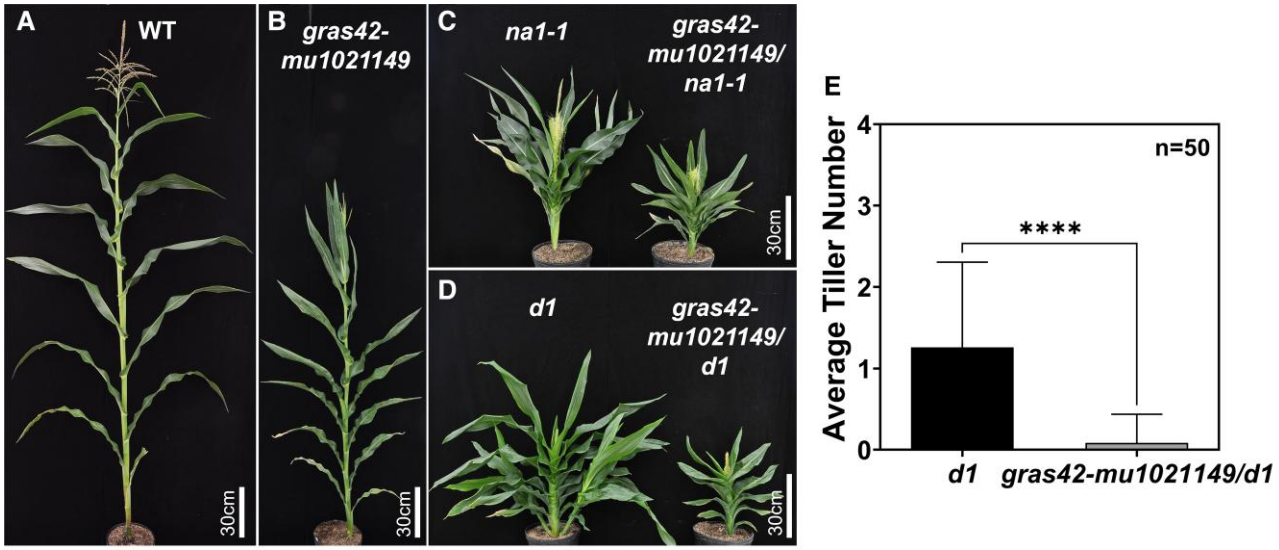

Figure 9. Phenotype of single and double mutants. **A)** Plant height of mature wild type (*gras42-mu1021149/+*) *gras42-mu1021149* homozygote; **B)** Plant height of *na1-1* and *gras42-mu1021149/na1-1* double mutant; **C)** Plant height and tillers of *d1* and *gras42-mu1021149/d1* double mutant; **D)** Average number of tillers in *d1* and *gras42-mu1021149/d1* double mutant. Error bars are ± SD. Asterisks represents a significant difference between *d1* and *gras42-mu1021149/d1* determined by student's t-test. (**** = $P < 0.0001$).

and often exhibit the presence of pistils in the tassel florets. The *d1* mutant a GA-deficient dwarf due to loss of *ent*-kaurene synthase activity, an early step in GA biosynthesis (Fu et al. 2016). The *d1* dwarfs display an increase in the number of tillers and retention of anthers in the pistillate flowers of the ear. Both *na1-1* and *d1* single mutants are severely reduced in height as compared to the wild type. Previous work demonstrated context-dependent genetic interactions between BR and GA deficiency (Best et al. 2016). GA and BR were additive for plant height, the increased branching of GA mutants required BR, and the tassel phenotypes in BR-deficient mutants required GA (Best et al. 2016). Based on the expression analysis, we expect *gras42-mu1021149* to behave like a weak loss of BR mutant. If this is correct, *gras42-mu1021149* should recapitulate the interactions described previously by enhancing the retention of pistils in the *na1-1* mutant and reducing the number of tillers in the *d1* mutant. If it is a GA signaling mutant, on the other hand, we should observe an increase in tillers in *d1* and a suppression of pistil retention in *na1-1* tassels.

Double-mutant phenotypes between *gras42-mu1021149* and *na1-1* or *d1* were consistent with *gras42-mu1021149* affecting a weak loss of BR signaling. As compared to all single mutants, plant height was reduced even further in the *gras42-mu1021149/na1-1* and *gras42-mu1021149/d1* double mutants indicating an additive effect of these mutations on height (Fig. 9). Previous findings have shown that BR biosynthetic mutants could suppress the tillering induced by GA mutants (Best et al. 2016). Like other BR mutants, *gras42-mu1021149* completely suppressed the tillering induced by *d1* in *gras42-mu1021149/d1* double mutants (Fig. 9). Thus, just like BR-deficient dwarfs (Best et al. 2016) *gras42* is required for loss of GA to induce tillering. Although the *gras42-mu1021149* tassels did not exhibit any silks, loss of *GRAS42* in the *gras42-mu1021149/na1-1* double mutants enhanced the penetrance of the persistence of pistils in the tassel florets (Fig. 10). No normal tassels were observed in *gras42-mu1021149/na1-1* double mutants. Ninety-two percent of the *gras42-mu1021149/na1-1* tassels had silks, and the remainder were barren (Fig. 10). Some *gras42-mu1021149* single mutant tassels exhibited barren branches (Fig. 10) as was observed in GA excess treatments (Best and Dilkes 2022). All *gras42-mu1021149/d1* tassels were completely normal demonstrating that *d1* suppresses the *gras42-mu1021149* barren phenotype and that, just as was the case for the presence of pistils in the tassel for BR-deficient mutants, GA is required for the *gras42-mu1021149* tassel phenotype. It has been previously shown that GA can induce male sterility in maize (Nelson and Rossman 1958; Best and Dilkes 2022). The suppression of the barren phenotype by *gras42-mu1021149/d1* double mutants indicates that the male sterility in *gras42-mu1021149* may be due to excess GA in this tissue. In summary, *gras42-mu1021149* enhanced the height impacts of both *na1-1* and *d1* mutants, enhanced the retention of pistils in the tassel florets of *na1-1*, suppressed the increased branching of GA deficiency, and exhibited a barren tassel phenotype that required GA. Thus, *gras42-mu1021149* and its interactions closely resemble a loss of BR signaling.

Expression level polymorphism discovery via genome-wide association for the GRAS42 transcript

To identify natural variants regulating the expression of the *gras42* gene, we performed an expression level genome-wide association study (eGWAS) using published

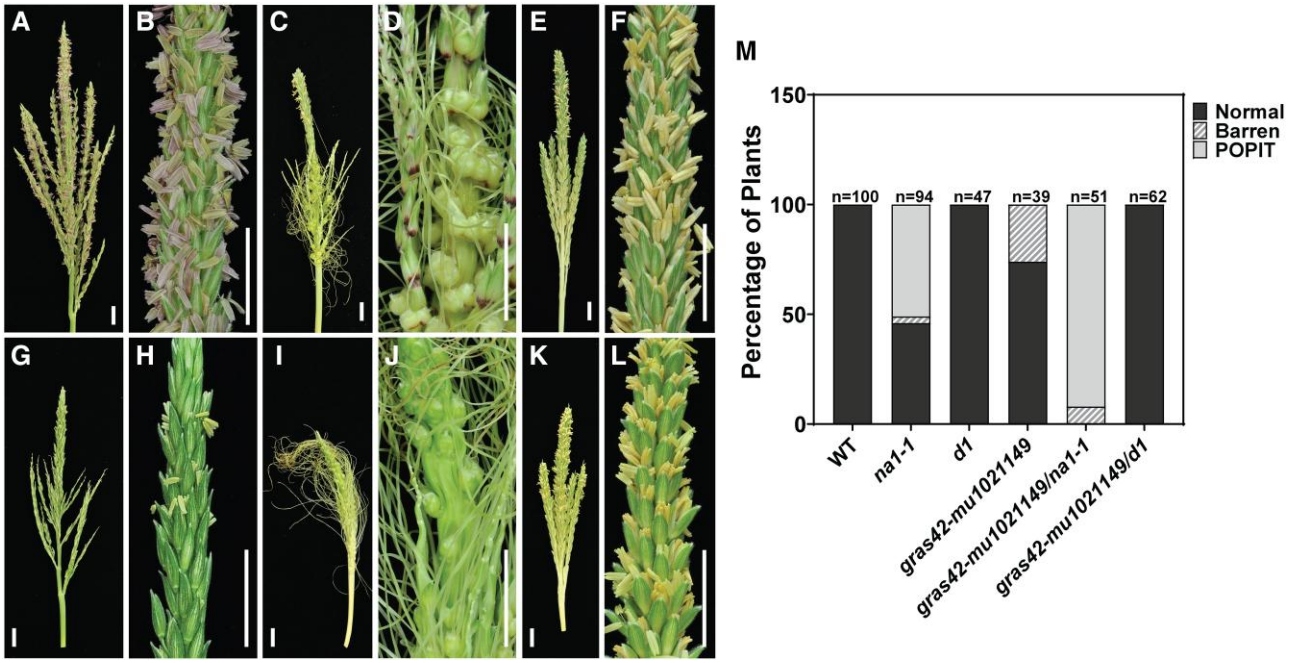

Figure 10. Tassel phenotype in single and double mutants. **A–B)** WT (*gras42-mu1021149/+*); **C–D)** *na1-1*; **E–F)** *d1*; **G–H)** *gras42-mu1021149*; **I–J)** *gras42-mu1021149/na1-1*; **K–L)** *gras42-mu1021149/d1*. Scale bars = 2 cm; **M)** Percentage of plants showing normal, barren tassels and presence of pistil in tassel (POPIT) phenotypes in WT and mutants (*n* = number of plants).

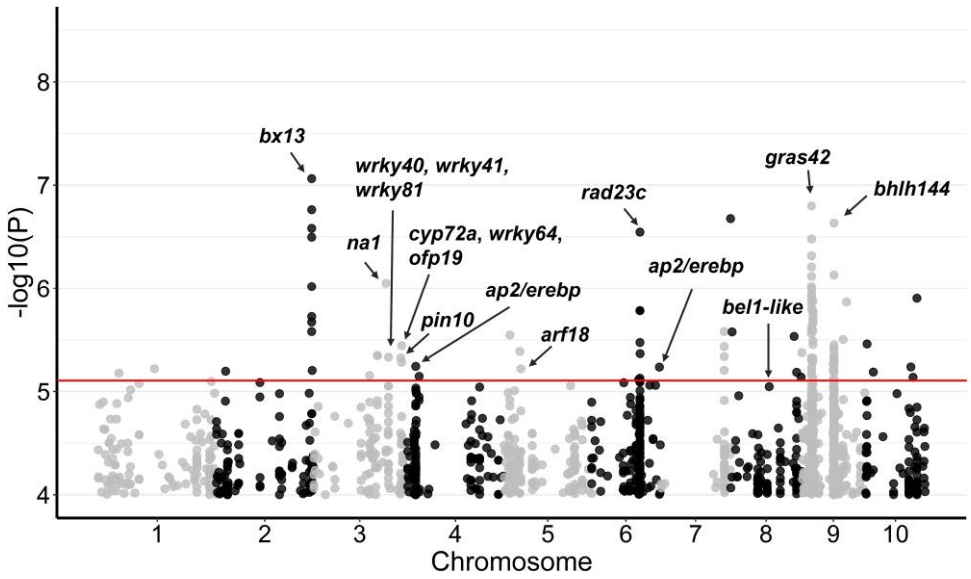

Figure 11. Manhattan plot for eGWAS of *gras42* expression in 296 maize diverse lines. The dots represent SNPs associated with *gras42* gene expression. Red line is the *P*-value (*P*) threshold selected to identify significant associations. The black arrows highlight selected potential candidate genes of interest.

data from RNA-seq of seedling shoots from 296 inbred lines (Kremling et al. 2018). This identified 153 SNPs with a *P*-value <1E-5 for accumulation of the GRAS42 transcript (Fig. 11). Among these SNPs, 19 were located within 1 Mb of the *gras42* gene and likely identified *cis*-acting regulatory variation (Fig. 11, Supplementary Table S6).

In addition to the *cis*-eQTLs, 134 alleles had trans effects on GRAS42 accumulation (Fig. 11, Table 4, Supplementary Table S6). Among these, eight SNPs on chromosome 2 were associated with *benzoxazinone synthesis13* (*bx13*, Zm00001d007718). One of the trans-acting SNPs was located in a region containing the previously discussed BR biosynthetic gene *na1*. Two SNPs were located in a

Table 4. Candidate genes for selected trans regulators of GRAS42 accumulation from genome-wide analysis (GWA) of expression level in germinating shoots

SNP_ID	CHR	POS	SNP Effect	*P*-value	Candidate genes	Annotation
2-238126834	2	238126834	0.256559263	2.63E-06	Zm00001d007718	*benzoxazinone synthesis13* (*bx13*)
2-238126871	2	238126871	0.269199382	3.19E-07		
2-238126877	2	238126877	0.249651008	1.88E-06		
2-238126885	2	238126885	0.261970019	9.63E-07		
2-238126887	2	238126887	0.252683244	2.13E-06		
2-238126898	2	238126898	0.27493553	1.73E-07		
2-238126917	2	238126917	0.27870554	2.62E-07		
2-238126921	2	238126921	0.287780931	8.64E-08		
3-181905371	3	181905371	0.231101747	8.92E-07	Zm00001d042843	*nana plant1*
3-187852439	3	187852439	0.305093516	4.66E-06	Zm00001d043060	*wrky81, wrky40, wrky41*
3-187852502	3	187852502	0.299513231	8.84E-06		
3-218581094	3	218581094	−0.434818966	4.74E-06	Zm00001d044083	*pin-formed protein10*
3-220839119	3	220839119	0.308542162	3.60E-06	Zm00001d044159,	*cyp72a, wrky64, ovate family protein 19*
3-220839454	3	220839454	0.279605606	5.22E-06	Zm00001d044162, Zm00001d044167	
4-25786156	4	25786156	0.332474966	5.72E-06	Zm00001d049309	AP2/EREBP transcription factor family protein
4-25793512	4	25793512	0.328920312	9.77E-06		
5-43614831	5	43614831	0.304801044	6.04E-06	Zm00001d014377	*auxin response factor 18*
6-121088509	6	121088509	0.256423203	7.45E-06	Zm00001d037326	*ubiquitin receptor rad23c*
6-121105526	6	121105526	0.308627916	2.85E-07		
6-121109485	6	121109485	0.269018031	3.36E-06		
6-169631183	6	169631183	−0.216194592	5.81E-06	Zm00001d039077	AP2/EREBP transcription factor family protein
8-97557162	8	97557162	0.460036521	8.99E-06	Zm00001d010060	*bel1-like homeodomain protein 9*
9-24602648	9	24602648	0.253305497	9.62E-07	Zm00001d045499	E3 ubiquitin-protein ligase XBAT33
9-24602809	9	24602809	−0.219449999	2.74E-06		
9-24602814	9	24602814	−0.214284656	4.73E-06		
9-80799902	9	80799902	0.214318727	4.63E-06	Zm00001d046332	Transcription factor *bhlh144*
9-80799911	9	80799911	0.215975058	3.90E-06		
9-80800029	9	80800029	0.20923684	8.17E-06		
9-80804330	9	80804330	0.212343734	5.65E-06		
9-80845657	9	80845657	0.209586406	7.60E-06		
9-80856131	9	80856131	0.230804504	7.42E-07		
9-80872311	9	80872311	0.213091242	5.22E-06		
9-80872445	9	80872445	0.206834285	1.00E-05		
9-80876041	9	80876041	0.212724836	6.18E-06		
9-80882352	9	80882352	0.210570565	8.17E-06		
9-80887549	9	80887549	0.240565074	2.33E-07		
9-80887566	9	80887566	0.207684343	9.17E-06		
9-80903148	9	80903148	0.213727359	4.90E-06		
9-80903157	9	80903157	0.215941274	3.87E-06		
9-80903168	9	80903168	0.215941274	3.87E-06		
10-21259279	10	21259279	0.224851277	6.49E-06	Zm00001d023795	E3 ubiquitin-protein ligase UPL1

locus with three potential candidate genes: *cyp72a/cyp11* (Zm00001d044159), *wrky64* (Zm00001d044162), and *ovate family protein19* (*ofp19*, Zm00001d044167). The *cyp72a* gene is a homolog of Arabidopsis *CYP72C1* that likely controls BR homeostasis (Thornton et al. 2010). Gene *ofp19* is a homolog of rice *OsOFP2*. Ovate family proteins are transcription repressors know to interact with DLT in rice and are involved in modulating BR responses through this interaction (Xiao et al. 2017; Yang et al. 2018). The *wrky64* gene encodes a homolog of *AtWRKY71* that controls shoot branching in Arabidopsis by regulating the auxin pathway. Another locus on chromosome 8 was linked to *bel1 like homeodomain protein 9* (Zm00001d010060) which is orthologous to the *REPLUMLESS* (aka *PENNYWISE/BELLRINGER/VAAMANA/LARSON*) gene in Arabidopsis which is known to control meristem maintenance, internode patterning, and flowering through interaction with KNOX genes (Kanrar et al. 2006). In addition to *wrky64* on chromosome 3, we identified three SNPs adjacent to a cluster of WRKY transcription factors (Zm00001d043060, Zm00001d043062, Zm00001d043063, and Zm00001d043066). Among these, Zm00001d043060 is an ortholog of AtWRKY70 and AtWRKY54, both of which are positive regulators of the BR pathway in Arabidopsis (Chen et al. 2017). We also identified SNPs linked to *pin-formed protein10* (*pin10*), a putative auxin efflux carrier encoded by Zm00001d044083, and *auxin response factor18* (*arf18*, Zm00001d014377) as potential candidates affecting GRAS42 accumulation in our eGWAS. In addition, ubiquitin receptor *rad23c* (Zm00001d037326), E3 ubiquitin-protein ligase *xbat33* (Zm00001d045499) and E3

ubiquitin ligase *upl1* (Zm00001d023795) were identified as potential candidate genes affecting the accumulation of GRAS42. Overlap of *trans*-acting eGWAS loci with the *gras42* co-expressed genes identified from the single-cell expression analysis (Supplementary Table S4) was worse than expected by random chance, indicating that co-expression did not enrich for regulators of *gras42* expression. Together this suggests that BR, auxin, and protein turnover pathways may all influence the accumulation of GRAS42 in maize.

Discussion

In this study we report a semi-dwarf maize mutant, *gras42-mu1021149*. We identified three mutant alleles of *gras42* in the maize ortholog of the rice *DLT* and Arabidopsis *SCL28* genes. A mutator transposon insertion allele, *gras42-mu1021149*, was characterized in depth. The mutant has short dark green leaves, upright leaf angles, reduced tillering, and partially barren tassel branches (Fig. 1 and Fig. 10). The phenotype of loss of *gras42* is consistent with that reported for *dlt* loss-of-function mutants in rice (Tong et al. 2009; Li et al. 2010) and resembles some of the known BR-deficient mutants of maize (Hartwig et al. 2011; Best et al. 2016). The *Mu* insertion in *gras42-mu1021149* resulted in the accumulation of truncated transcripts corresponding to the first third of the gene up to the *Mu* insertion site. Reads downstream from the *Mu* insertion were also detected, though at much lower levels, and their accumulation was consistent with the ectopic promoter activity of *Mu* responding to the regulatory environment of *gras42* (Supplementary Fig. S2). Prior study found a similar pattern in other Mu insertions (Ellison et al. 2023). A systematic analysis of aberrant transcripts from *Mu* insertions would determine whether this observation is an unusual anecdote or an aspect of *Mu*'s biology.

Differential gene expression analysis by RNA-seq suggests that *gras42* could determine leaf angle via regulation of KNOX transcription factors and auxin levels. We identified transcripts of two class I KNOX family genes, *lg3* and *rs1*, that increased in the *gras42-mu1021149* RNA-seq data from stem and SAM tissue. The likely auxin biosynthetic gene, *yucca6*, was also downregulated in *gras42-mu1021149*. In addition, an early auxin-responsive gene, *aas6*, was differentially expressed in *gras42-mu1021149*. *AAS6* is a putative auxin amido synthase gene in the GH3 family which is also known to regulate leaf angle in rice (Zhao et al. 2013; Zhang et al. 2015). The accumulation of GRAS42 in cells undergoing the G2/M transition in shoot apices (Fig. 3) suggests that these regulatory events may occur during or concomitant with the modulation of cell division patterns early in organ development.

Maize GRAS42 regulates BR response

The semi-dwarf stature of the *gras42-mu1021149* mutant resembled the expected phenotype from weak BR deficiency. An analysis of gene expression was consistent with a loss of BR signaling in *gras42-mu1021149*. Expression changes in known BR-responsive genes were used as indicators of BR pathway activation in *gras42-mu1021149*. Gene expression changes at BR-responsive genes in *gras42-mu1021149* resembled a loss of BR response in the mutant. The expression pattern in both of our actively growing tissues: stem and SAM and expanding leaf sheaths were consistent with a weak loss of BR response in *gras42-mu1021149* (Tables 1 and 2). This was also evident using a parametric index calculated from the expression effects on BR-responsive genes. Loss of *gras42-mu1021149* increased the transcript levels of BR-repressed genes and decreased the transcripts of BR-induced genes (Fig. 7). The examination of gene expression consequences of loss of *gras42-mu1021149* indicates that GRAS42 acts as a positive regulator of BR-responsive gene expression. During the drafting of this manuscript, Wang et al. (2022) showed that *Zm*BZR1 (aka BZR1, GRMZM5G812774, Zm00001d046305, Zm0001eb384820) and *Zm*BEH1 (aka BES1, GRMZM2G102514, Zm00001d02197, Zm00001eb325550) bind to the promoter of *gras42* (Wang et al. 2022). Working with the same *gras42-mu1021149* allele, Wang et al. (2022) showed that these maize mutants are semi-dwarf and have more upright leaves than wild-type siblings. In rice, the orthologous gene, *DLT*, interacts with OSH15 to regulate the expression of the BR receptor, BRI1, and BR catabolizing enzyme CYP734A5/6 (Niu et al. 2022). These results demonstrate that GRAS42 plays roles both upstream and downstream of BR signaling. This is consistent with our finding that GRAS acts as positive regulator of BR-responsive gene expression.

Our double-mutant interactions were also consistent with *gras42* encoding a positive regulator of BR-responsive gene expression. The enhanced penetrance of the presence of pistils in the tassel florets of *gras42-mu1021149/na1-1* double mutants is consistent with weak loss of BR signaling in *gras42-mu1021149* (Fig. 10). The *gras42* gene was required for BRs to suppress pistils in tassel florets suggesting a role of *gras42* in BR signaling. Furthermore, *gras42-mu1021149* suppressed tillering in *gras42-mu1021149/d1* double mutants indicating that *gras42* is required for loss of GA to induce tillering (Fig. 9). This is consistent with the suppression of tillering observed due to loss of BR in double mutants defective in GA and BR biosynthesis (Best et al. 2016). In addition, the previously observed requirement for GA production for pistil production in tassel florets of BR-deficient plants (Best et al. 2016, 2017), the GA-deficient mutant *d1* suppressed the tassel phenotype of *gras42-mu1021149* (Fig. 10). Taken together, these findings show that *gras42* positively affects BR signaling which is consistent with previous reports with the role of *DLT* in rice (Tong et al. 2009, 2012; Yang et al. 2018). However, unlike studies in rice, we did not observe consistent alterations in the expression of BR biosynthetic or core signaling genes in maize *gras42-mu1021149* mutants (Fig. 5 and Supplementary Fig. S5). The *gras42-mu1021149* mutants exhibit or enhance every phenotype associated with a loss BR biosynthesis including plant height, retention of pistils in tassel florets, and suppression of tiller outgrowth in GA loss-of-function

mutants (Fig. 1, Fig. 9, and Fig. 10). However, this effect is context dependent and tissues in which GRAS42 is not accumulated (e.g. mature leaf tissue, Fig. 4) were not impacted for BR-regulated gene expression while rapidly expanding tissues were (Table 1 and 2 and Fig. 7).

Does GRAS42 regulate the GA pathway?

Two opposing roles for DLT in the regulation of the GA pathway were previously proposed from work in rice. In one study, the levels of GA biosynthetic genes were increased in rice *dlt* mutants (Li et al. 2010). In a second study, the accumulation of transcripts encoding a GA catabolic gene was increased and transcripts encoding two GA biosynthetic genes were unaffected in rice *dlt* mutants (Tong et al. 2014). We did not observe consistent changes in transcript levels of GA biosynthetic genes in our three RNA-seq experiments (Fig. 5 and Supplementary Fig. S5). We also did not see consistent changes in the levels of GA-regulated gene expression in our three RNA-seq experiments (Table 3 and Fig. 8). The only GA biosynthetic gene differentially expressed in any RNA-seq comparison between *gras42-mu1021149* and wild-type siblings was *d3*, and that was only differentially expressed in the stem and SAM tissue (Fig. 5). In addition, the expression levels of core GA signaling genes were not consistently impacted in *gras42-mu1021149* (Fig. 5 and Supplementary Fig. S5). This demonstrates that GRAS42 is not a primary regulator of GA biosynthesis and signaling in maize. We did observe an increase in the transcript levels of GA catabolic enzymes (GA2OX) in *gras42-mu1021149* stem and SAM tissue (Fig. 5), similar to the Tong et al. (2014) study, but this effect was not consistent across tissues. The finding of coordinated accumulation of GA-regulated genes by *gras42-mu1021149* in our RNA-seq experiments, but with opposite effects depending on the tissue, is similar to the context-dependent epistatic interactions between BR and GA biosynthetic mutants in maize (Best et al. 2016) that was confirmed using hormone biosynthetic inhibitors (Best et al. 2017).

We used hormone-regulated gene sets to examine the state of signaling across our different tissues and genotypes. These composite values, indices, derived from the expression of a set of genes report on the status of hormone response. Gene expression indices calculated using the set of genes affected by BR excess demonstrate active BR signaling in actively dividing stem and SAM as well as expanding leaf sheaths of wild-type plants (Fig. 7). However, a reversal in this pattern was observed in already expanded L3 base suggesting that expanded leaves have suppressed or no BR signaling. These finding are consistent with the tissue-specific distribution of BR biosynthesis reported previously (Shimada et al. 2003). Our data reveals that this tissue specificity also extends to BR responses. Tissue dependency was also detected in GA responses using indices calculated in the three tissues using the set of genes affected by GA excess. In contrast to high BR response in stem including SAM, a low GA response was detected in this tissue in the wild-type plants. While the expanding leaf sheath showed active GA signaling, no response was detected in L3 base. Since the GA and BR responses are variable across tissues, it further suggests that mechanisms of interaction between the two hormones are tissue-specific and *gras42* may influence this through interaction with other transcription factors.

The responses to loss of *gras42* were also tissue-specific. Different sets of genes were differentially expressed in stem and L3 base. In addition, expression analysis of specific gene sets showed opposite responses in the actively growing and already expanded tissues. For instance, *gras42-mu1021149* led to an increase in transcript levels of *ga2oxidases* in stem and SAM but a decrease in *ga2oxidases* was observed in L3 base (Fig. 5). This flipping of gene expression consequences between tissues was also evident from the transcript levels of BR- and GA-responsive genes. The distribution of the two sets of BR-repressed genes (leaf and shoot) in *gras42-mu1021149* L3 base indicated a gain of BR response in this tissue which is the opposite of what we observe in the other two tissues (Tables 2 and 3). Similarly, the pattern of GA-induced genes in L3 base contrasts to that in the other two tissues indicating a tissue-specific role of *gras42*. These differences could be attributed to GRAS42 expression levels in the three tissues (Fig. 4) and/or tissue-specific protein interactors. Given the absence of GRAS42 transcripts in L3 base, it is likely that effects in this tissue are secondary effects mediated by variation in mobile signals produced in other parts of the plant.

GRAS42 is unlikely to be the mediator of previously reported tissue-specific epistatic interactions between hormone biosynthetic mutants

As both the wild type and *gras42-mu1021149* showed a reversal in BR-responsive gene expression across tissues this suggests that *gras42* is not the mediator of the reversed effects between stem, leaf sheaths, and leaf blades (Fig. 7). This opposite effect of gene regulation in a tissue-specific manner is a function of the genes influenced by BR, rather than the effect of *gras42-mu1021149* on BR-regulated gene expression. This suggests the existence of a repressor or activator that drives a reversal in the transcriptional control of BR-regulated genes as maize leaf tissue moves from a rapidly expanding and dividing developmental state to maturity. This unknown factor may also be responsible for the reversions in the direction epistatic interactions between BR and GA biosynthetic mutants (Best et al. 2016). The large number of BZR paralogs in maize (Manoli et al. 2018), which may have undergone expression sub functionalization and diverged in protein function, are candidates for the mediators of the differential effects of BR on gene expression between maize tissues.

In this study, we demonstrated that maize *gras42* affects both BR- and GA-responsive gene expression in a tissue-specific manner. However, many of these changes are unlikely to be direct. Analysis of previously published single-cell transcriptomic data found *GRAS42* transcripts substantially enriched among dividing cells in the shoot apex (Fig. 3). Together with the hormone responsive gene expression analysis, this suggests that *gras42* encodes a repressor of BR signaling that acts during cell proliferation. The role for BR in

cell cycle regulated gene expression and cell division has been known for decades (Hu et al. 2000; Nakaya et al. 2002; Oakenfull et al. 2002). Previous analyses of BR consequences on cell division have been mixed, but promotion of cell division and cell cycle regulated gene expression has been demonstrated when BR-deficient cells are supplied with exogenous BR (Hu et al. 2000). Though BR excess can also inhibit cell divisions and growth, particularly in root tissues where sub-nanomolar application enhances root growth and greater concentrations inhibit growth. BR has also been implicated in the cell divisions that precede stomatal development in Arabidopsis (Gudesblat et al. 2012; Kim et al. 2012; Wang et al. 2015). The relationship between BR and stomatal development is unclear and complicated by tissue and species-specific effects (Qi and Torii 2018). Though co-expression was detected between GRAS42 and TMM1 and ZmSPCH2 in our analysis of public single-cell data (Supplementary Fig. S1), no differences in stomatal densities or index were observed in the BR-deficient mutant *na2* (Best et al. 2016) suggesting that this hormone is not required for normal stomatal development in maize.

The rice ortholog of *gras42*, DLT has previously been reported to be co-regulated with BZR1 by GSK2 in rice, placing it downstream of GSK2 in BR signaling (Tong et al. 2012). BZR1 has also been shown to bind to the *gras42* promoter in maize and rice (Tong et al. 2009; Wang et al. 2022). Our data show that *gras42* does not regulate expression of BR biosynthetic genes but does affect the expression of BR-responsive genes (Fig. 5 and Fig. 7). In addition, the expression of *brassinozole resistant1* (*bzr1*, Zm00001d046305) and other upstream BR signaling genes like Arabidopsis *BAK1* homolog *somatic embryogenesis receptor-like kinase2 -like1* (*serk2l1*, Zm00001d024430) and *brassinosteroid insensitive1-associated receptor kinase like3* (*bak3*, Zm00001d037010) were not affected by loss of *gras42* (Fig. 5 and Supplementary Fig. S5). These results are consistent with *gras42* acting downstream of *BZR1* in regulating the transcriptional response to BR. On the other hand, DLT has been shown to modulate the expression of GA biosynthetic genes in rice (Li et al. 2010), but its role in GA signaling has not been defined. The expression of GA biosynthetic genes was not affected in maize *gras42-mu1021149*, but expression of GA-induced genes was affected by loss of *gras42*. Considering that GA-induced gene expression changes are DELLA dependent, it may be that GRAS42 interacts with DELLAs to modulate GA signaling. We propose that *gras42* might be responsible for mediating cross-talk between the BR and GA pathway by interacting with BZR1 and DELLA transcription factors.

Natural variation in GRAS42 transcript accumulation places it downstream of BR

The eGWAS analysis revealed that the expression of *gras42* was associated with SNPs linked to known components of the BR pathway, including BR biosynthesis (*na1*), degradation (*cyp72A*), and signaling (WRKY transcription factor Zm00001d043060). The *ofp19* gene was also identified as a putative candidate regulating the accumulation of GRAS42. OFPs regulate plant growth and development through their interactions with multiple transcription factors. Interactions between OFPs and DLT have been previously reported in rice (Xiao et al. 2017; Yang et al. 2018). OFPs are also known to interact with KNOX and BEL1-like homeodomain (BELL) proteins and suppress the BELL-KNOX heterodimers (Pagnussat et al. 2007; Liu and Douglas 2015; Zhang et al. 2016). A *bell9* (Zm00001d010060) gene was identified as a potential regulator of GRAS42 expression in our eGWAS analysis. OFPs have also been shown to function in hormone signaling. OsOFP8 is phosphorylated by GSK2 and plays and role in BR signaling (Yang et al. 2016). The OFPs are also known to affect leaf angle. Gain-of-function mutant *Osofp8* and *OsOFP8* overexpression lines showed increased leaf angle, whereas the leaf angle was more upright in *OsOFP8* RNAi transgenic lines. The finding that *ofp19* regulates GRAS42 expression raises the possibility that OFPs function through interaction with GRAS42 in determining leaf inclination.

Materials and methods

Plant material

The maize (*Zea mays*) Robertson's *Mutator* (*Mu*) allele of *gras42*, *gras42-mu1021149* (aka *url1-1*, *scl28-1*, *bcr1-1*, and UFMu-09491) (McCarty et al. 2005; Hartwig 2011; Wang et al. 2022) was identified in the Uniform-*Mu* population (McCarty et al. 2005). An additional allele of *gras42* (*gras42-3*, *url1-2*, *bcr1-2*) was identified from a spontaneous mutant in the CML247 inbred line which failed to complement *gras42-1* (Hartwig 2011). An EMS allele, *gras42-4*, was identified within a family used by the maize TILLInG project (Till et al. 2004; Weil and Monde 2007) which was segregating for a semi-dwarf that also failed to complement *gras42-mu1021149*. The *dwarf1 (d1)* allele was obtained from Carolina biological supply. The *nana plant1-1* (*na1-1*) mutant was described previously (Hartwig et al. 2011). To generate the double mutants, pollen from homozygous *na1-1* and homozygous *d1* mutants was used in crosses to *gras42-mu1021149* homozygotes. The resulting F_1 plants were selfed and subsequent F_2 families were grown and phenotyped for tillering, plant height, and persistence of pistils in the tassels.

Growth conditions

Greenhouse experiments measuring the growth and development of single and double mutants were conducted at the Purdue Horticulture Plant Growth Facility using a 16:8 hr day: night cycle provided by supplemental lighting with temperature settings of 27°C (day) and 21°C (night). Plants were grown in 100% Turface MVP (Profile Products, Inc.) and fertilized with 200 ppm Nitrogen mixed from a 21-5-20 N-P-K mix (Miracle-Gro Excel, Scotts, Marysville, OH) and adjusted to pH 6.

Morphological measurements

Plant height of 20 *gras42-mu1021149* heterozygote and 20 homozygote siblings were measured every 7 d starting at

26 d after planting and continued until maturity. Height was measured as the distance from the soil surface to the top-most visible developed leaf collar.

Leaf numbers for *gras42-mu1021149* heterozygote and homozygote siblings were counted at maturity. Since the lower leaves undergo senescence before plants reach maturity, every second leaf was marked counting the first developing true leaf as one. Leaf length and width were measured after leaves were fully extended. The distance from the leaf collar to the tip along the midrib was measured for the leaf length, whereas the widest point of the leaf was selected for leaf width measurements.

The leaf angles of *gras42-mu1021149* mutants and heterozygous siblings were measured with a digital protractor (WR400 3-inch goniometer, Wixey, Sanibel, FL). The angle between the stem and the abaxial side of the midrib was determined after plants reached maturity (post-anthesis). The inclination angle, the acute angle between the leaf and the stem above the leaf, is reported.

Genotyping

The molecular identity of the *gras42-4* allele was determined using Illumina sequencing of the overlapping PCR amplicons covering the entire *gras42* locus (Supplementary Table S7). This approach, known as wideseq, has been previously described in Khangura et al. 2019. Briefly, PCR products from a single mutant individual spanning the entire gene were pooled and prepared for sequencing using the Tn5-tagmentation procedure with the Illumina Nextera DNA library preparation kit. These libraries were sequenced using a MiSeq instrument (Illumina, San Diego, CA) at the Purdue Genomics Core Facility. Paired-end reads from each sample were processed to remove adapters and poor quality bases (<Phred-20) using Trimmomatic version 0.22 (Bolger et al. 2014) with the following settings "LEADING:20 TRAILING:20 MINLEN:30". Only the filtered paired reads were used for further processing. The filtered paired-end reads were aligned to the *gras42* genomic sequence using short read aligner BWA version 0.7.12 (Li and Durbin 2009). The alignments were generated using the BWA *sampe* command with default parameters to generate Sequence Alignment/Map (SAM) files. The SAM files were converted into Binary Alignment Map (BAM) files, followed by sorting, indexing, and finally, variant calling using *mpileup* function in SAMtools suite version 1.3 (Li et al. 2009). The variants were also manually inspected by visualizing each sample in IGV version 2.8.2 (Thorvaldsdottir et al. 2013) using the sorted BAM files.

The single-nucleotide substitution (G221A) in *gras42-4* was followed by PCR and cleavage of amplicons with a restriction endonuclease. This mutation created an AvrII restriction site 5′-C^CT***A***GG-3′, from 5′-CCT***G***GG-3′ creating a co-dominant Cleaved Amplified Polymorphic Sequence (CAPS) (Konieczny and Ausubel 1993). Primer pair URL-F2 and URL-R2 (Supplementary Table S7) produced a 797 bp amplicon encompassing the AvrII restriction site. The PCR products were digested with AvrII restriction endonuclease followed by electrophoresis on a 2.5% (w/v) agarose gel could distinguish the wild-type allele as an undigested amplicon of 797 bp and *gras42-4* allele as two bands at 642 and 155 bp.

The genotyping of individuals segregating for the *gras42-mu1021149* allele was done using *gras42-specific* primer pairs URL-F2 and URL-R2, along with a *Mutator* TIR-specific primer Eomu3 (Supplementary Table S7) to create two dominant markers. Individuals with the *gras42-mu1021149* allele produced a PCR amplicon when tested with Eomu3 and URL-F2 or URL-R2 primer pairs. The wild-type allele was successfully amplified by the URL-F2 and URL-R2 primer pair.

RNA sequencing and transcriptome analysis

Three tissue types including stem, leaf sheathes from the expanding leaves, and base of the third collared leaf (L3 base) were collected from heterozygous and homozygous *gras42-mu1021149* seedlings at V3 developmental stage. The one-inch stem sections comprised the stem, shoot apical meristem (SAM), and the surrounding leaf sheaths. Heterozygous and homozygous plants collected as three replicates of 12 plants each. Total RNA was extracted using TRIzol reagent. The concentration and quality of the RNA was measured using a Nanodrop 2000c spectrophotometer (Thermo Scientific, Waltham, MA). Library construction and sequencing were performed by Novogene using the NovaSeq 6000 sequencing platform (Illumina, San Diego, CA).

The reads were aligned to the maize reference genome (Zm-B73-REFERENCE-GRAMENE-4.0) using hisat2 (Kim et al. 2019). The aligned reads for each sample were individually assembled using cufflinks (Trapnell et al. 2012). Transcript assemblies generated by cufflinks were merged by cuffmerge. The count files containing number of aligned reads corresponding to each gene were generated using htseq-count (Anders et al. 2015). DEGs were called using DEseq2 version 1.26.0 (Love et al. 2014). DEseq2 results for the three tissues are available in Supplementary Table S8. Transcripts with $|\log_2 \text{fold change}| \geq 1$ and FDR adjusted P-value ≤ 0.05 were considered as DEGs (Supplementary Table S2).

Analysis of published single-cell RNA-seq

A public dataset from Satterlee et al. (2020) comprising two B73 replicates were obtained from NCBI (SRR11943512 and SRR11943513). Data were processed in Cell Ranger v6.0 (10× Genomics) making a custom reference genome and mapping to B73 maize genome version 5. A raw gene counts matrix was used as an input to detect empty droplets using DropletUtils v1.16 (Lun et al. 2019). After filtering out empty droplets, the gene counts matrix was imported to the Seurat v4 package, following Seurat standard pipeline (Hao et al. 2021). High quality cells were considered to have less than 5% of mitochondrial expressed genes, more than 2,500 genes detected per cell, and less than 100,000 transcripts detected per cell. Data were transformed using the *SCTransform* function, which was followed by dimensionality reduction and

cell clustering. Different cell clusters were identified with previously published marker genes (Satterlee et al. 2020). Cell cycle scoring was performed to identify clusters undergoing cell division process. Data generated with Seurat were exported using the package SeuratWrappers to an appropriate format for Monocle. Using Monocle v4, we identified modules with co-regulated genes through a graph-autocorrelation analysis (Cao et al. 2019).

Phylogenetic analysis

The protein sequences for GRAS42 homologs in amborella (*Amborella trichopoda*), asparagus (*Asparagus officinalis*), garlic (*Allium sativum*), Arabidopsis (*Arabidopsis thaliana*), brachypodium (*Brachypodium distachyon*), rice (*Oryza sativa* ssp. *japonica*), setaria (*Setaria italica* and *Setaria viridis*), and sorghum (*Sorghum bicolor*) were obtained from the Plaza monocot 5.0 databases (Van Bel et al. 2022). The sequences were aligned using clustalW (Larkin et al. 2007) with default parameters (Gap opening penalty: 10 and gap extension cost: 0.20). A maximum-likelihood tree was estimated using IQ-TREE version 1.5.5 (Nguyen et al. 2015) with substitution model JTT + I + G4 as the best predicted model by Bayesian information criteria (Kalyaanamoorthy et al. 2017). A consensus tree was generated using ultrafast bootstrapping with 1000 replicates (Minh et al. 2013). The tree was visualized using iTOL v6 (Letunic and Bork 2021).

Gene set enrichment/chi-square test

Publicly available data were utilized to obtain BR- and GA-affected gene sets. The genes differentially expressed in leaf and shoot tissues of maize seedlings treated with 1 nM epibrassinolide were obtained from Trevisan et al. 2020. The DEG sets were divided into two subsets of upregulated and downregulated genes for each tissue. These were named BR-induced and BR-repressed genes, respectively. The DEGs in leaf sheaths of V3 maize seedlings treated with 10^{-4} M GA_3 were obtained from a previous study (Wang et al. 2019) and grouped into GA-induced and GA-repressed gene sets. The normalized counts of genes in a set were extracted from our wild type and *gras42-mu1021149* RNA sequencing data for all the three tissues (stem and SAM, expanding leaf sheaths, and L3 base). The effect of *gras42-mu1021149* on the expression of a gene set was analyzed using a chi-squared test. The expected proportion of up and downregulated genes was calculated based on the distribution of induced and repressed genes among all expressed genes, not just the DEG sets, in each experiment.

Index calculation

A Z-score was calculated for each gene from the normalized counts in three replicates each of wild type and *gras42-mu1021149*. The Z-score of each gene for each sample was calculated as follows:

$$\text{Z-score}_{\text{geneA}} = \frac{\textit{Normalized counts of gene A} - \textit{Average counts of gene A in WT and mutant}}{\textit{Standard Deviation}}$$

An index was then generated for each sample by taking the average of the Z-scores for the set of BR- and GA-regulated genes described above.

eGWAS

The normalized counts of GRAS42 transcripts in germinating shoot tissue from 296 maize diversity lines were obtained from RNA sequencing performed in a previous study (Kremling et al. 2018). The SNP data for these lines were obtained from maize Hapmap3.2.1 (Bukowski et al. 2018). The SNP data were filtered for minor allele frequency (MAF) $\leq$ 0.05, and 23.9 M SNPs were retained. For genome-wide association, we modified the R package switchgrassGWAS (Lovell et al. 2021) to adapt the bigsnpr R package (Privé et al. 2018) for maize. The results were filtered to retain SNPs below a *P*-value of 1E-5 as significantly associated with *gras42* expression. The SNPs within 1 Mb of the *gras42* translation start site or the *gras42* stop codon were considered cis-acting and the rest of the SNPs were considered trans-acting. Within the candidate locus, three genes upstream and three genes downstream from the SNP position were considered as potential candidates associated with the SNP. GWAS results were viewed using an interactive browser: Zbrowse (Ziegler et al. 2015). The annotations for the candidate genes were obtained from several sources including Gramene, MaizeGDB (https://www.maizegdb.org; Portwood et al. 2019; Woodhouse et al. 2021a) and JGI genome portal (https://genome.jgi.doe.gov/portal/).

Accession numbers

The accession numbers for major genes/proteins from this article can be found in Supplementary Table S3, Table S7, and Table S9.

Acknowledgments

The authors would like to acknowledge the assistance of the staff and leadership at the Agronomy Center for Research and Education, Rosen Center for Advanced Computing, and the Horticulture Greenhouse at Purdue University. We are grateful to Dilkes lab members for comments and discussions. We would particularly like to thank everyone who puts extra effort into scientific software documentation and data dissemination that allows research such as this to determine meaning from open-source repositories. In particular, the

NSF Cyverse project, Alice MacQueen, and Tom Juenger, and the labs of Ed Buckler, Yao Chen, and Serena Varotto—you are the real heroes.

Author contributions

A.K., N.B.B., T.H., R.S.K., B.S., and B.P.D. designed the research. A.K., N.B.B., T.H., J.B., R.S.K., S.M., A.A.-R., J.S., B.S., and B.P.D. performed the experiments and analyzed data. A.K., N.B.B., T.H., R.S.K., A.A.-R., and B.P.D. wrote the paper. All authors edited and approved the manuscript.

Supplementary data

The following materials are available in the online version of this article.

Supplementary Figure S1. Density plots of maize genes.

Supplementary Figure S2. BAM coverage and alignment of reads that span *gras42* gene in stem and SAM tissue.

Supplementary Figure S3. BAM coverage and alignment of reads that span *gras42* gene in stem and SAM tissue in expanding leaf sheaths.

Supplementary Figure S4. Phylogenetic tree for GRAS42 protein homologs

Supplementary Figure S5. Circle plot showing $\log_2$ fold change of sterol and brassinosteroid (BR) biosynthetic genes, BR signaling genes, and gibberellin (GA) biosynthetic and signaling genes.

Supplementary Table S1. Expression (FPKM) of *gras42* and *gras47* across different maize tissues obtained from qTeller.

Supplementary Table S2. Differentially expressed genes (DEGs) in *gras42-mu1021149* stem and SAM and L3 base tissues.

Supplementary Table S3. Normalized counts of maize *smr* genes in WT and *gras42-mu1021149* in three tissues: stem and SAM, expanding leaf sheaths and L3 base.

Supplementary Table S4. Genes co-expressed with *gras42* in single-cell transcriptomic data along with their $\log_2$ fold change in *gras42-mu1021149* vs WT.

Supplementary Table S5. Expression changes for genes encoding steps in brassinosteroid (BR) and gibberellin (GA) pathways in *gras42-mu1021149* mutant.

Supplementary Table S6. Cis and trans variants affecting GRAS42 transcript accumulation in germinating shoot at $P < 1E\text{-}5$.

Supplementary Table S7. Primer pairs used for genotyping of *gras42* alleles and wide seq.

Supplementary Table S8. DEseq2 output for *gras42-mu1021149* vs WT comparison in three tissues.

Supplementary Table S9. Gene IDs for maize, Arabidopsis and rice genes mentioned in the manuscript.

Funding

This work was supported by United States Department of Agriculture National Institute of Food and Agriculture postdoctoral grant 2022-67012-36601 to R.S.K. and United States Department of Energy Office of Science (BER) Grant DE-SC0023305 and National Science Foundation IOS-175 5401 to B.P.D. J.S. is supported by NCSU startup funds.

Conflict of interest statement. None declared.

Data availability

Raw reads from RNA sequencing of *gras42-mu1021149* homozygote and heterozygote siblings in three tissues generated and analyzed in this study are available at NCBI Sequence Read Archive (SRA) under the bioproject accession number PRJNA831826.

References

Abendroth LJ, Elmore RW, Boyer MJ, Marlay SK. Corn growth and development. Ames: Iowa State University; 2011.

Anders S, Pyl PT, Huber W. HTSeq–a python framework to work with high-throughput sequencing data. Bioinformatics. 2015:**31**(2):166–169. https://doi.org/10.1093/bioinformatics/btu638

Aoi Y, Tanaka K, Cook SD, Hayashi KI, Kasahara H. GH3 auxin-amido synthetases alter the ratio of indole-3-acetic acid and phenylacetic acid in Arabidopsis. Plant Cell Physiol. 2020:**61**(3):596–605. https://doi.org/10.1093/pcp/pcz223

Bage SA, Barten TJ, Brown AN, Crowley JH, Deng M, Fouquet R, Gomez JR, Hatton TW, Lamb JC, LeDeaux JR, et al. Genetic characterization of novel and CRISPR-cas9 gene edited maize brachytic 2 alleles. Plant Gene. 2020:**21**:100198. https://doi.org/10.1016/j.plgene.2019.100198

Becraft PW, Freeling M. Genetic analysis of rough sheath1 developmental mutants of maize. Genetics. 1994:**136**(1):295–311. https://doi.org/10.1093/genetics/136.1.295

Bensen RJ, Johal GS, Crane VC, Tossberg JT, Schnable PS, Meeley RB, Briggs SP. Cloning and characterization of the maize an1 gene. Plant Cell. 1995:**7**(1):75. https://doi.org/10.1105/tpc.7.1.75

Best NB, Dilkes BP. Transcriptional responses to gibberellin in the maize tassel and control by DELLA domain proteins. Plant J. 2022:**112**(2):493–517. https://doi.org/10.1111/tpj.15961

Best NB, Hartwig T, Budka J, Fujioka S, Johal G, Schulz B, Dilkes BP. *nana plant2* encodes a maize ortholog of the Arabidopsis brassinosteroid biosynthesis gene *DWARF1*, identifying developmental interactions between brassinosteroids and gibberellins. Plant Physiol. 2016:**171**(4):2633–2647. https://doi.org/10.1104/pp.16.00399

Best NB, Johal G, Dilkes BP. Phytohormone inhibitor treatments phenocopy brassinosteroid–gibberellin dwarf mutant interactions in maize. Plant Direct. 2017:**1**(2):pld3.9. https://doi.org/10.1002/pld3.9

Bolduc N, Tyers RG, Freeling M, Hake S. Unequal redundancy in maize *knotted1 homeobox* genes. Plant Physiol. 2014:**164**(1):229–238. https://doi.org/10.1104/pp.113.228791

Bolger AM, Lohse M, Usadel B. Trimmomatic: a flexible trimmer for illumina sequence data. Bioinformatics. 2014:**30**(15):2114–2120. https://doi.org/10.1093/bioinformatics/btu170

Bukowski R, Guo X, Lu Y, Zou C, He B, Rong Z, Wang B, Xu D, Yang B, Xie C, et al. Construction of the third-generation *Zea mays* haplotype map. Gigascience. 2018:**7**(4):1–12. https://doi.org/10.1093/gigascience/gix134

Cao J, Spielmann M, Qiu X, Huang X, Ibrahim DM, Hill AJ, Zhang F, Mundlos S, Christiansen L, Steemers FJ, et al. The single-cell transcriptional landscape of mammalian organogenesis. Nature. 2019:**566**(7745):496–502. https://doi.org/10.1038/s41586-019-0969-x

Cao Y, Zhong Z, Wang H, Shen R. Leaf angle: a target of genetic improvement in cereal crops tailored for high-density planting. Plant Biotechnol J. 2022:**20**(3):426–436. https://doi.org/10.1111/pbi.13780

Chen Y, Hou M, Liu L, Wu S, Shen Y, Ishiyama K, Kobayashi M, McCarty DR, Tan B-C. The maize DWARF1 encodes a gibberellin 3-oxidase and is dual localized to the nucleus and cytosol. Plant Physiol. 2014:**166**(4):2028–2039. https://doi.org/10.1104/pp.114.247486

Chen J, Nolan T, Ye H, Zhang M, Tong H, Xin P, Chu J, Chu C, Li Z, Yin Y. Arabidopsis WRKY46, WRKY54 and WRKY70 transcription factors are involved in brassinosteroid-regulated plant growth and drought response. Plant Cell. 2017:**29**:tpc.00364.2017. https://doi.org/10.1105/tpc.17.00364

Chung Y, Choe S. The regulation of brassinosteroid biosynthesis in Arabidopsis. CRC Crit Rev Plant Sci. 2013:**32**(6):396–410. https://doi.org/10.1080/07352689.2013.797856

Clouse SD. Brassinosteroid signal transduction: from receptor kinase activation to transcriptional networks regulating plant development. Plant Cell. 2011:**23**(4):1219–1230. https://doi.org/10.1105/tpc.111.084475

Duvick DN. Genetic progress in yield of United States maize (*Zea mays* L). Maydica. 2005:**50**:193.

Ellison EL, Zhou P, Hermanson P, Chu YH, Read A, Hirsch CN, Grotewold E, Springer NM. Mutator transposon insertions within maize genes often provide a novel outward reading promoter. Genetics. 2023:**225**(3):iyad171. https://doi.org/10.1093/genetics/iyad171

Fowler JE, Freeling M. Genetic analysis of mutations that alter cell fates in maize leaves: DominantLiguleless mutations. Dev Genet. 1996:**18**(3):198–222. https://doi.org/10.1002/(SICI)1520-6408(1996)18:3<198::AID-DVG2>3.0.CO;2-4

Fu J, Ren F, Lu X, Mao H, Xu M, Degenhardt J, Peters RJ, Wang Q. A tandem array of *ent* -kaurene synthases in maize with roles in gibberellin and more specialized metabolism. Plant Physiol. 2016:**170**(2):742–751. https://doi.org/10.1104/pp.15.01727

Goldy C, Pedroza-Garcia J-A, Breakfield N, Cools T, Vena R, Benfey PN, De Veylder L, Palatnik J, Rodriguez RE. The *Arabidopsis* GRAS-type SCL28 transcription factor controls the mitotic cell cycle and division plane orientation. Proc Natl Acad Sci U S A. 2021:**118**(6):e2005256118. https://doi.org/10.1073/pnas.2005256118

Gudesblat GE, Schneider-Pizoń J, Betti C, Mayerhofer J, Vanhoutte I, van Dongen W, Boeren S, Zhiponova M, de Vries S, Jonak C, et al. SPEECHLESS integrates brassinosteroid and stomata signalling pathways. Nat Cell Biol. 2012:**14**(5):548–554. https://doi.org/10.1038/ncb2471

Guo Y, Wu H, Li X, Li Q, Zhao X, Duan X, An Y, Lv W, An H. Identification and expression of GRAS family genes in maize (*Zea mays* L). PLoS One. 2017:**12**(9):e0185418. https://doi.org/10.1371/journal.pone.0185418

Hao Y, Hao S, Andersen-Nissen E, Mauck WM, Zheng S, Butler A, Lee MJ, Wilk AJ, Darby C, Zager M, et al. Integrated analysis of multimodal single-cell data. Cell. 2021:**184**(13):3573–3587.e29. https://doi.org/10.1016/j.cell.2021.04.048

Hartwig T. Functional characterization of brassinosteroid mutants in maize. Doctoral dissertation. Purdue University, West Lafayette 2011

Hartwig T, Chuck GS, Fujioka S, Klempien A, Weizbauer R, Potluri DP, Choe S, Johal GS, Schulz B. Brassinosteroid control of sex determination in maize. Proc Natl Acad Sci U S A. 2011:**108**(49):19814–19819. https://doi.org/10.1073/pnas.1108359108

Hirano K, Yoshida H, Aya K, Kawamura M, Hayashi M, Hobo T, Sato-Izawa K, Kitano H, Ueguchi-Tanaka M, Matsuoka M. SMALL ORGAN SIZE 1 and SMALL ORGAN SIZE 2/DWARF AND LOW-TILLERING form a complex to integrate auxin and brassinosteroid signaling in rice. Mol Plant. 2017:**10**(4):590–604. https://doi.org/10.1016/j.molp.2016.12.013

Hu Y, Bao F, Li J. Promotive effect of brassinosteroids on cell division involves a distinct CycD3-induction pathway in Arabidopsis. Plant J. 2000:**24**(5):693–701. https://doi.org/10.1046/j.1365-313x.2000.00915.x

Hu X, Qian Q, Xu T, Zhang Y, Dong G, Gao T, Xie Q, Xue Y. The U-box E3 ubiquitin ligase TUD1 functions with a heterotrimeric G α subunit to regulate brassinosteroid-mediated growth in rice. PLoS Genet. 2013:**9**(3):e1003391. https://doi.org/10.1371/journal.pgen.1003391

Hutchison CB. The linkage of certain aleurone and endosperm factors in maize, and their relation to other linkage groups. Ithaca (NY): Cornell University; 1922.

Jeong IK, Sharkhuu A, Jing BJ, Li P, Jae CJ, Baek D, Sang YL, Blakeslee JJ, Murphy AS, Bohnert HJ, et al. Yucca6, a dominant mutation in arabidopsis, affects auxin accumulation and auxin-related phenotypes. Plant Physiol. 2007:**145**(3):722–735. https://doi.org/10.1104/pp.107.104935

Jiang F, Guo M, Yang F, Duncan K, Jackson D, Rafalski A, Wang S, Li B. Mutations in an AP2 transcription factor-like gene affect internode length and leaf shape in maize. PLoS One. 2012:**7**(5):e37040. https://doi.org/10.1371/journal.pone.0037040

Kalyaanamoorthy S, Minh BQ, Wong TKF, von Haeseler A, Jermiin LS. ModelFinder: fast model selection for accurate phylogenetic estimates. Nat Methods. 2017:**14**(6):587–589. https://doi.org/10.1038/nmeth.4285

Kanrar S, Onguka O, Smith HMS. Arabidopsis inflorescence architecture requires the activities of KNOX-BELL homeodomain heterodimers. Planta. 2006:**224**(5):1163–1173. https://doi.org/10.1007/s00425-006-0298-9

Khangura RS, Marla S, Venkata BP, Heller NJ, Johal GS, Dilkes BP. A *Very Oil Yellow1* modifier of the *Oil Yellow1-N1989* allele uncovers a cryptic phenotypic impact of *Cis* -regulatory variation in maize. G3 Genes|Genomes|Genetics. 2019:**9**:375–390. https://doi.org/10.1534/g3.118.200798

Khush GS. Green revolution: the way forward. Nat Rev Genet. 2001:**2**:815–822. https://doi.org/10.1038/35093585

Kim T-W, Michniewicz M, Bergmann DC, Wang Z-Y. Brassinosteroid regulates stomatal development by GSK3-mediated inhibition of a MAPK pathway. Nature. 2012:**482**:419–422. https://doi.org/10.1038/nature10794

Kim D, Paggi JM, Park C, Bennett C, Salzberg SL. Graph-based genome alignment and genotyping with HISAT2 and HISAT-genotype. Nat Biotechnol. 2019:**37**:907–915. https://doi.org/10.1038/s41587-019-0201-4

Kim E-J, Russinova E. Brassinosteroid signalling. Curr Biol. 2020:**30**:R294–R298. https://doi.org/10.1016/j.cub.2020.02.011

Kir G, Ye H, Nelissen H, Neelakandan AK, Kusnandar AS, Luo A, Inzé D, Sylvester AW, Yin Y, Becraft PW. RNA interference knockdown of BRASSINOSTEROID INSENSITIVE1 in maize reveals novel functions for brassinosteroid signaling in controlling plant architecture. Plant Physiol. 2015:**169**:826–839. https://doi.org/10.1104/pp.15.00367

Konieczny A, Ausubel FM. A procedure for mapping Arabidopsis mutations using co-dominant ecotype-specific PCR-based markers. Plant J. 1993:**4**:403–410. https://doi.org/10.1046/j.1365-313X.1993.04020403.x

Kremling KAG, Chen SY, Su MH, Lepak NK, Romay MC, Swarts KL, Lu F, Lorant A, Bradbury PJ, Buckler ES. Dysregulation of expression correlates with rare-allele burden and fitness loss in maize. Nature. 2018:**555**:520–523. https://doi.org/10.1038/nature25966

Lambert RJ, Johnson RR. Leaf angle, tassel morphology, and the performance of maize hybrids. Crop Sci. 1978:**18**:499–502. https://doi.org/10.2135/cropsci1978.0011183X001800030037x

Larkin MA, Blackshields G, Brown NP, Chenna R, McGettigan PA, McWilliam H, Valentin F, Wallace IM, Wilm A, Lopez R, et al. Clustal W and clustal X version 2.0. Bioinformatics. 2007:**23**:2947–2948. https://doi.org/10.1093/bioinformatics/btm404

Letunic I, Bork P. Interactive tree of life (iTOL) v5: an online tool for phylogenetic tree display and annotation. Nucleic Acids Res. 2021:**49**:W293–W296. https://doi.org/10.1093/nar/gkab301

Li HW. HERITABLE CHARACTERS IN MAIZE. J Hered. 1933:**24**:279–281. https://doi.org/10.1093/oxfordjournals.jhered.a103798

Li H, Durbin R. Fast and accurate short read alignment with Burrows-Wheeler transform. Bioinformatics. 2009:**25**:1754–1760. https://doi.org/10.1093/bioinformatics/btp324

Li H, Handsaker B, Wysoker A, Fennell T, Ruan J, Homer N, Marth G, Abecasis G, Durbin R. The sequence alignment/map format and

SAMtools. Bioinformatics. 2009:**25**:2078–2079. https://doi.org/10.1093/bioinformatics/btp352

Li X, Wu P, Lu Y, Guo S, Zhong Z, Shen R, Xie Q. Synergistic interaction of phytohormones in determining leaf angle in crops. Int J Mol Sci. 2020:**21**:5052. https://doi.org/10.3390/ijms21145052

Li W, Wu J, Weng S, Zhang Y, Zhang D, Shi C. Identification and characterization of dwarf 62, a loss-of-function mutation in DLT/OsGRAS-32 affecting gibberellin metabolism in rice. Planta. 2010:**232**:1383–1396. https://doi.org/10.1007/s00425-010-1263-1

Lindstrom EW. Genetical research with maize. Genetica. 1923:**5**:327–356. https://doi.org/10.1007/BF01508815

Liu Y, Douglas CJ. A role for OVATE FAMILY PROTEIN1 (OFP1) and OFP4 in a BLH6-KNAT7 multi-protein complex regulating secondary cell wall formation in Arabidopsis thaliana. Plant Signal Behav. 2015:**10**:e1033126. https://doi.org/10.1080/15592324.2015.1033126

Liu G, Hou P, Xie R, Ming B, Wang K, Xu W, Liu W, Yang Y, Li S. Canopy characteristics of high-yield maize with yield potential of 22.5 Mg ha−1. Field Crops Res. 2017:**213**:221–230. https://doi.org/10.1016/j.fcr.2017.08.011

Love MI, Huber W, Anders S. Moderated estimation of fold change and dispersion for RNA-seq data with DESeq2. Genome Biol. 2014:**15**:550. https://doi.org/10.1186/s13059-014-0550-8

Lovell JT, MacQueen AH, Mamidi S, Bonnette J, Jenkins J, Napier JD, Sreedasyam A, Healey A, Session A, Shu S, et al. Genomic mechanisms of climate adaptation in polyploid bioenergy switchgrass. Nature. 2021:**590**(7846):438–444. https://doi.org/10.1038/s41586-020-03127-1

Lun ATL, Riesenfeld S, Andrews T, Dao TP, Gomes T, Marioni JC. EmptyDrops: distinguishing cells from empty droplets in droplet-based single-cell RNA sequencing data. Genome Biol. 2019:**20**:63. https://doi.org/10.1186/s13059-019-1662-y

Makarevitch I, Thompson A, Muehlbauer GJ, Springer NM. Brd1 gene in maize encodes a brassinosteroid C-6 oxidase. PLoS One. 2012:**7**:30798. https://doi.org/10.1371/journal.pone.0030798

Manoli A, Trevisan S, Quaggiotti S, Varotto S. Identification and characterization of the BZR transcription factor family and its expression in response to abiotic stresses in *Zea mays* L. Plant Growth Regul. 2018:**84**:423–436. https://doi.org/10.1007/s10725-017-0350-8

McCarty DR, Mark Settles A, Suzuki M, Tan BC, Latshaw S, Porch T, Robin K, Baier J, Avigne W, Lai J, et al. Steady-state transposon mutagenesis in inbred maize. Plant J. 2005:**44**:52–61. https://doi.org/10.1111/j.1365-313X.2005.02509.x

Minh BQ, Nguyen MAT, von Haeseler A. Ultrafast approximation for phylogenetic bootstrap. Mol Biol Evol. 2013:**30**:1188–1195. https://doi.org/10.1093/molbev/mst024

Moreno MA, Harper LC, Krueger RW, Dellaporta SL, Freeling M. Liguleless1 encodes a nuclear-localized protein required for induction of ligules and auricles during maize leaf organogenesis. Genes Dev. 1997:**11**:616–628. https://doi.org/10.1101/gad.11.5.616

Muehlbauer GJ, Fowler JE, Girard L, Tyers R, Harper L, Freeling M. Ectopic expression of the maize homeobox gene *Liguleless3* alters cell fates in the leaf1. Plant Physiol. 1999:**119**:651–662. https://doi.org/10.1104/pp.119.2.651

Multani DS. Loss of an MDR transporter in compact stalks of maize br2 and Sorghum dw3 mutants. Science. 2003:**302**(5642):81–84. https://doi.org/10.1126/science.1086072

Nakaya M, Tsukaya H, Murakami N, Kato M. Brassinosteroids control the proliferation of leaf cells of Arabidopsis thaliana. Plant Cell Physiol. 2002:**43**:239–244. https://doi.org/10.1093/pcp/pcf024

Nelson PM, Rossman EC. Chemical induction of male sterility in inbred maize by use of gibberellins. Science. 1958:**127**(3313):1500–1501. https://doi.org/10.1126/science.127.3313.1500-a

Nguyen L-T, Schmidt HA, von Haeseler A, Minh BQ. IQ-TREE: a fast and effective stochastic algorithm for estimating maximum-likelihood phylogenies. Mol Biol Evol. 2015:**32**:268–274. https://doi.org/10.1093/molbev/msu300

Niu M, Wang H, Yin W, Meng W, Xiao Y, Liu D, Zhang X, Dong N, Liu J, Yang Y, et al. Rice DWARF AND LOW-TILLERING and the homeodomain protein OSH15 interact to regulate internode elongation via orchestrating brassinosteroid signaling and metabolism. Plant Cell. 2022:**34**:3754–3772. https://doi.org/10.1093/plcell/koac196

Nomoto Y, Takatsuka H, Yamada K, Suzuki T, Suzuki T, Huang Y, Latrasse D, An J, Gombos M, Breuer C, et al. A hierarchical transcriptional network activates specific CDK inhibitors that regulate G2 to control cell size and number in Arabidopsis. Nat Commun. 2022:**13**:1660. https://doi.org/10.1038/s41467-022-29316-2

Oakenfull EA, Riou-Khamlichi C, Murray AH. Plant D–type cyclins and the control of G1 progression. Philos Trans R Soc Lond B Biol Sci. 2002:**357**:749–760. https://doi.org/10.1098/rstb.2002.1085

Ohnishi T, Godza B, Watanabe B, Fujioka S, Hategan L, Ide K, Shibata K, Yokota T, Szekeres M, Mizutani M. CYP90A1/CPD, a brassinosteroid biosynthetic cytochrome P450 of Arabidopsis, catalyzes C-3 oxidation. J Biol Chem. 2012:**287**(37):31551–31560. https://doi.org/10.1074/jbc.M112.392720

Paciorek T, Chiapelli BJ, Wang JY, Paciorek M, Yang H, Sant A, Val DL, Boddu J, Liu K, Gu C, et al. Targeted suppression of gibberellin biosynthetic genes ZmGA20ox3 and ZmGA20ox5 produces a short stature maize ideotype. Plant Biotechnol J. 2022:**20**:1140–1153. https://doi.org/10.1111/pbi.13797

Pagnussat GC, Yu H-J, Sundaresan V. Cell-Fate switch of synergid to egg cell in *Arabidopsis eostre* mutant embryo sacs arises from misexpression of the BEL1-like homeodomain gene *BLH1*. Plant Cell. 2007:**19**:3578–3592. https://doi.org/10.1105/tpc.107.054890

Phillips KA, Skirpan AL, Liu X, Christensen A, Slewinski TL, Hudson C, Barazesh S, Cohen JD, Malcomber S, McSteen P. *Vanishing tassel2* encodes a grass-specific tryptophan aminotransferase required for vegetative and reproductive development in maize. Plant Cell. 2011:**23**:550–566. https://doi.org/10.1105/tpc.110.075267

Portwood JL, Woodhouse MR, Cannon EK, Gardiner JM, Harper LC, Schaeffer ML, Walsh JR, Sen TZ, Cho KT, Schott DA, et al. MaizeGDB 2018: the maize multi-genome genetics and genomics database. Nucleic Acids Res. 2019:**47**:D1146–D1154. https://doi.org/10.1093/nar/gky1046

Privé F, Aschard H, Ziyatdinov A, Blum MGB. Efficient analysis of large-scale genome-wide data with two R packages: bigstatsr and bigsnpr. Bioinformatics. 2018:**34**:2781–2787. https://doi.org/10.1093/bioinformatics/bty185

Qi X, Torii KU. Hormonal and environmental signals guiding stomatal development. BMC Biol. 2018:**16**:21. https://doi.org/10.1186/s12915-018-0488-5

Qiao S, Sun S, Wang L, Wu Z, Li C, Li X, Wang T, Leng L, Tian W, Lu T, et al. The RLA1/SMOS1 transcription factor functions with OsBZR1 to regulate brassinosteroid signaling and rice architecture. Plant Cell. 2017:**29**:292–309. https://doi.org/10.1105/tpc.16.00611

Salas Fernandez MG, Becraft PW, Yin Y, Lübberstedt T. From dwarves to giants? Plant height manipulation for biomass yield. Trends Plant Sci. 2009:**14**:454–461. https://doi.org/10.1016/j.tplants.2009.06.005

Satterlee JW, Strable J, Scanlon MJ. Plant stem-cell organization and differentiation at single-cell resolution. Proc Natl Acad Sci U S A. 2020:**117**(52):33689–33699. https://doi.org/10.1073/PNAS.2018788117

Shimada Y, Goda H, Nakamura A, Takatsuto S, Fujioka S, Yoshida S. Organ-specific expression of brassinosteroid-biosynthetic genes and distribution of endogenous brassinosteroids in Arabidopsis. Plant Physiol. 2003:**131**:287–297. https://doi.org/10.1104/pp.013029

Tanaka A, Nakagawa H, Tomita C, Shimatani Z, Ohtake M, Nomura T, Jiang C-J, Dubouzet JG, Kikuchi S, Sekimoto H, et al. *BRASSINOSTEROID UPREGULATED1*, encoding a helix-loop-helix protein, is a novel gene involved in brassinosteroid signaling and controls bending of the lamina joint in rice. Plant Physiol. 2009:**151**:669–680. https://doi.org/10.1104/pp.109.140806

Thornton LE, Rupasinghe SG, Peng H, Schuler MA, Neff MM. Arabidopsis CYP72C1 is an atypical cytochrome P450 that inactivates brassinosteroids. Plant Mol Biol. 2010:**74**:167–181. https://doi.org/10.1007/s11103-010-9663-y

Thorvaldsdottir H, Robinson JT, Mesirov JP. Integrative genomics viewer (IGV): high-performance genomics data visualization and exploration. Brief Bioinform. 2013:**14**:178–192. https://doi.org/10.1093/bib/bbs017

Tian J, Wang C, Xia J, Wu L, Xu G, Wu W, Li D, Qin W, Han X, Chen Q, et al. Teosinte ligule allele narrows plant architecture and enhances high-density maize yields. Science. 2019:**365**(6454):658–664. https://doi.org/10.1126/science.aax5482

Till BJ, Reynolds SH, Weil C, Springer N, Burtner C, Young K, Bowers E, Codomo CA, Enns LC, Odden AR, et al. Discovery of induced point mutations in maize genes by TILLING. BMC Plant Biol. 2004:**4**(1):12. https://doi.org/10.1186/1471-2229-4-12

Tong H, Jin Y, Liu W, Li F, Fang J, Yin Y, Qian Q, Zhu L, Chu C. DWARF and LOW-TILLERING, a new member of the GRAS family, plays positive roles in brassinosteroid signaling in rice. Plant J. 2009:**58**:803–816. https://doi.org/10.1111/j.1365-313X.2009.03825.x

Tong H, Liu L, Jin Y, Du L, Yin Y, Qian Q, Zhu L, Chu C. DWARF AND LOW-TILLERING acts as a direct downstream target of a GSK3/SHAGGY-like kinase to mediate brassinosteroid responses in rice. Plant Cell. 2012:**24**:2562–2577. https://doi.org/10.1105/tpc.112.097394

Tong H, Xiao Y, Liu D, Gao S, Liu L, Yin Y, Jin Y, Qian Q, Chu C. Brassinosteroid regulates cell elongation by modulating gibberellin metabolism in rice. Plant Cell. 2014:**26**:4376–4393. https://doi.org/10.1105/tpc.114.132092

Trapnell C, Roberts A, Goff L, Pertea G, Kim D, Kelley DR, Pimentel H, Salzberg SL, Rinn JL, Pachter L. Differential gene and transcript expression analysis of RNA-Seq experiments with TopHat and cufflinks. Nat Protoc. 2012:**7**:562–578. https://doi.org/10.1038/nprot.2012.016

Trevisan S, Forestan C, Brojanigo S, Quaggiotti S, Varotto S. Brassinosteroid application affects the growth and gravitropic response of maize by regulating gene expression in the roots, shoots and leaves. Plant Growth Regul. 2020:**92**:117–130. https://doi.org/10.1007/s10725-020-00626-z

Van Bel M, Silvestri F, Weitz EM, Kreft L, Botzki A, Coppens F, Vandepoele K. PLAZA 5.0: extending the scope and power of comparative and functional genomics in plants. Nucleic Acids Res. 2022:**50**:D1468–D1474. https://doi.org/10.1093/nar/gkab1024

Walsh J, Waters CA, Freeling M. The maize gene *liguleless2* encodes a basic leucine zipper protein involved in the establishment of the leaf blade–sheath boundary. Genes Dev. 1998:**12**:208–218. https://doi.org/10.1101/gad.12.2.208

Wang Y, Wang X, Deng D, Wang Y. Maize transcriptomic repertoires respond to gibberellin stimulation. Mol Biol Rep. 2019:**46**:4409–4421. https://doi.org/10.1007/s11033-019-04896-3

Wang X, Wang X, Sun S, Tu X, Lin K, Qin L, Wang X, Li G, Zhong S, Li P. Characterization of regulatory modules controlling leaf angle in maize. Plant Physiol. 2022:**190**:500–515. https://doi.org/10.1093/plphys/kiac308

Wang M, Yang K, Le J. Organ-specific effects of brassinosteroids on stomatal production coordinate with the action of *TOO MANY MOUTHS*. J Integr Plant Biol. 2015:**57**:247–255. https://doi.org/10.1111/jipb.12285

Weil CF, Monde R. Getting the point—mutations in maize. Crop Sci. 2007. https://doi.org/10.2135/cropsci2006.09.0563tpg

Winkler RG, Helentjaris T. The maize Dwarf3 gene encodes a cytochrome P450-mediated early step in Gibberellin biosynthesis. Plant Cell. 1995:**7**:1307–1317. https://doi.org/10.1105/tpc.7.8.1307

Winkler Rodney G, Freeling M. Physiological genetics of the dominant gibberellin-nonresponsive maize dwarfs, Dwarf8 and Dwarf9. Planta. 1994:**193**(3):BF00201811. https://doi.org/10.1007/BF00201811

Woodhouse MR, Cannon EK, Portwood JL, Harper LC, Gardiner JM, Schaeffer ML, Andorf CM. A pan-genomic approach to genome databases using maize as a model system. BMC Plant Biol. 2021a:**21**(1):385. https://doi.org/10.1186/s12870-021-03173-5

Woodhouse MR, Sen S, Schott D, Portwood JL, Freeling M, Walley JW, Andorf CM, Schnable JC. Qteller: a tool for comparative multigenomic gene expression analysis. Bioinformatics. 2021b:**38**:236–242. https://doi.org/10.1093/bioinformatics/btab604

Xiao Y, Liu D, Zhang G, Tong H, Chu C. Brassinosteroids regulate OFP1, a DLT interacting protein, to modulate plant architecture and grain morphology in rice. Front Plant Sci. 2017:**8**:1698. https://doi.org/10.3389/fpls.2017.01698

Yang C, Ma Y, He Y, Tian Z, Li J. OsOFP19 modulates plant architecture by integrating the cell division pattern and brassinosteroid signaling. Plant J. 2018:**93**:489–501. https://doi.org/10.1111/tpj.13793

Yang C, Shen W, He Y, Tian Z, Li J. OVATE family protein 8 positively mediates brassinosteroid signaling through interacting with the GSK3-like kinase in rice. PLoS Genet. 2016:**12**:e1006118. https://doi.org/10.1371/journal.pgen.1006118

Yilmaz A, Nishiyama MY, Fuentes BG, Souza GM, Janies D, Gray J, Grotewold E. GRASSIUS: a platform for comparative regulatory genomics across the grasses. Plant Physiol. 2009:**149**:171–180. https://doi.org/10.1104/pp.108.128579

Zhang C, Bai M, Chong K. Brassinosteroid-mediated regulation of agronomic traits in rice. Plant Cell Rep. 2014:**33**:683–696. https://doi.org/10.1007/s00299-014-1578-7

Zhang S, Wang S, Xu Y, Yu C, Shen C, Qian Q, Geisler M, Jiang DA, Qi Y. The auxin response factor, OsARF19, controls rice leaf angles through positively regulating OsGH3-5 and OsBRI1. Plant Cell Environ. 2015:**38**:638–654. https://doi.org/10.1111/pce.12397

Zhang L, Zhang X, Ju H, Chen J, Wang S, Wang H, Zhao Y, Chang Y. Ovate family protein1 interaction with BLH3 regulates transition timing from vegetative to reproductive phase in Arabidopsis. Biochem Biophys Res Commun. 2016:**470**:492–497. https://doi.org/10.1016/j.bbrc.2016.01.135

Zhao S-Q, Xiang J-J, Xue H-W. Studies on the rice LEAF INCLINATION1 (LC1), an IAA–amido synthetase, reveal the effects of auxin in leaf inclination control. Mol Plant. 2013:**6**:174–187. https://doi.org/10.1093/mp/sss064

Ziegler GR, Hartsock RH, Baxter I. Zbrowse: an interactive GWAS results browser. PeerJ Comput Sci. 2015:**1**:e3. https://doi.org/10.7717/peerj-cs.3